Uncertainties in the adaptation of alpine pastures to climate change based on remote sensing products and modelling

L. Brilli, Raphaël Martin, G. Argenti, M. Bassignana, M. Bindi, R. Bonet, P. Choler, E. Cremonese, M. Della Vedova, C. Dibari, et al.

Uncertainties in the adaptation of alpine pastures to climate change based on remote sensing products and modelling

Brilli, L.[1,2]*, Martin, R.[3], Argenti, G.[2], Bassignana, M.[4], Bindi, M.[2], Bonet, R.[5], Choler, P.[6], Cremonese, E.[7], Della Vedova, M.[5], Dibari, C.[2], Filippa, G.[7], Galvagno, M.[7], Leolini, L.[2], Moriondo, M.[1,2], Piccot, A.[4], Stendardi, L.[2], Targetti, S.[8], Bellocchi, G.[3]

[1] National Research Council – Institute of BioEconomy (IBE-CNR) 50145 Sesto Fiorentino, Italy

[2] University of Florence, DAGRI, 50144 Florence, Italy

[3] Université Clermont Auvergne, INRAE, VetAgro Sup, UREP, 63000 Clermont-Ferrand, France

[4] Institut Agricole Régional, 11100 Aosta, Italy

[5] Parc National des Ecrins, Domaine de Charance, 05000 Gap, France

[6] Université Grenoble Alpes, Université Savoie Mont Blanc, CNRS, LECA, 38000 Grenoble, France

[7] Climate Change Unit, Environmental Protection Agency of Aosta Valley, Saint-Christophe, Italy

[8] University of Bologna, Department of Agricultural and Food Sciences, Viale Fanin, 50 - 40127 Bologna

*Corresponding author. Tel.: +39 0553033711

E-mail address: lorenzo.brilli@ibe.cnr.it (L. Brilli)

Highlights

- Alpine pastures are vulnerable to climate change.

- Remote sensing and modelling support vulnerability analysis in the western Alps.

- Earlier grazing, not changes in cattle density, copes with increased vulnerability.

- Summer water stresses and warming may lower C sequestration by pastures.

Abstract

Over the last century, the management of pastoral systems has undergone major changes to meet the livelihood needs of alpine communities. Faced with the changes induced by recent global warming, the ecological status of many pastoral systems has seriously deteriorated in the western alpine region. We assessed changes in pasture dynamics by integrating information from remote-sensing products and two process-based models, i.e. the grassland-specific, biogeochemical growth model PaSim and the generic crop-growth model DayCent. Meteorological observations and satellite-derived Normalised Difference Vegetation Index (NDVI) trajectories of three pasture macro-types (high, medium and low productivity classes) in two study areas - *Parc National des Écrins* (PNE) in France and *Parco Nazionale Gran Paradiso* (PNGP) in Italy - were used as a basis for the model calibration work. The performance of the models was satisfactory in reproducing pasture production dynamics (R^2=0.52 to 0.83). Projected changes in alpine pastures due to climate-change impacts and adaptation strategies indicate that: i) the length of the growing season is expected to increase between 15 and 40 days, resulting in changes in the timing and amount of biomass production, ii) summer water stress could limit pasture productivity; iii) earlier onset of grazing could enhance pasture productivity; iv) higher livestock densities could increase the rate of biomass regrowth, but major uncertainties in modelling processes need to be considered; and v) the carbon sequestration potential of pastures could decrease under limited water availability and warming.

Keywords: alpine pastures, climate-change adaptation, modelling, remote sensing

2

1.   Introduction

Mountain pastures are important livelihood systems in the European Alps, with a multifunctional form of land use encompassing agriculture, outdoor recreation, and tourism as well as conservation needs (Wanner et al., 2021). Rich in terms of biodiversity (Kurtogullari et al., 2020) and cultural heritage (Jourdain-Annequin and Duclos, 2006), alpine pastures fulfil economic, social and environmental functions at the same time (Bengtsson et al., 2019). They provide low-cost fodder for grazing livestock during the summer period and - where traditional transhumance systems are present – represent a complementary resource for Mediterranean pastoral systems (Caballero et al., 2009). Shaped by pastoral activities, alpine pastures have undergone multiple transformations over the centuries, mainly driven by the fragile balance between maximising agricultural productivity and the limits imposed by the temporal and spatial dynamics of the climate and forests-grasslands interactions (Kurz, 2013). However, alpine pastoralism manifests its fragility in the face of the changes induced by recent global warming. Climate changes and their impacts are visible in the alpine region, which has experienced a temperature increase of almost 2 °C over the last century, along with an important reduction of precipitation in the summer season (Gobiet et al., 2014). Specifically, droughts have been one of the main manifestations of climate variability. Corresponding to periods of abnormally low precipitation, they alter grassland productivity and quality (Nettier et al., 2010; Dibari et al., 2016) by offsetting the positive effect of summer heatwaves on canopy greenness (Corona-Lozada et al., 2019), as seen in the European Alps following a series of droughts (Calanca, 2007). The response of European mountain plant assemblages to increasing temperatures (thermophilisation) also suggests a progressive decline of cold-tolerant high-altitude grassland communities (Gottfried et al., 2012) and landscape modifications with warming-induced upward range shifts (Engler et al., 2011). This may lead to both a decrease in areas suitable for pasture and a reduction in pasture diversity driven by low-

3

73   quality vegetation types in the Alpine chain (Dibari et al., 2020), together with changes in grazing

74   practices (Dibari et al., 2021). This is critical because most impacts on grassland ecosystems can

75   be related to overgrazing and changes in the timing of livestock transhumance, with high stocking

76   densities in particular causing a range of negative impacts on plant and animal communities, as

77   observed in central France (Dumont et al., 2009) and in the Italian Maritime Alps (Negro et al.,

78   2011).

79   In this context, appropriate management can preserve grassland biodiversity, maintain socio-

80   ecological systems (Altaweel et al., 2015; Alessa et al., 2018) and counteract climate-change

81   impacts (Nori and Gemini, 2011; Felber et al., 2016). Specifically for the western Alps, global

82   warming and the increased frequency of extreme climate events such as heatwaves and droughts

83   have raised awareness of the need to adapt, due to the combined effects of climate and changes in

84   pastoral practices (Bonet et al., 2016). However, in many alpine zones, specific measures to

85   manage pastures in the face of climate change are still not implemented, despite the implementation

86   of agri-environmental and climate measures in the Common Agricultural Policy (EC, 2013). Since

87   proper management is needed to ensure the environmental, social and economic sustainability of

88   mountain permanent grasslands, a multi-disciplinary approach is a fundamental starting point,

89   involving the co-responsibility of livestock farmers and local officers, as well as cooperation based

90   on observation, modelling and intervention (Della-Vedova and Legeard, 2012).

91   This posture forms the basis of the design and implementation of this study started in 2017 in

92   two representative areas of the western alpine territory: the *Écrins* (France) and *Gran Paradiso*

93   (Italy) national parks (PNE and PNGP, respectively). In the pasturelands of the two parks, ground-

94   based and remotely sensed observation systems, as well as model-based simulations were used to

95   identify efficient management strategies able to support pastoral management and the sustainability

96   of pastoral systems. Modelling adaptation strategies was supported by a participatory-based

97 process bringing together different local stakeholders in the two case study areas. The target of the

98 modelling concerned the performance of pastoral systems and in particular the definition of

99 production while minimising environmental impacts. Remote sensing supports such modelling by

100 offering information on the spatial and temporal variation of important canopy state variables

101 which would be difficult to obtain otherwise. The involvement of local pastoralists was the basis

102 for the design and assessment of the analytical framework concerning the climate-change

103 adaptation strategies.

104   In the context of these alpine pastures, the objectives of this study were: (1) to inform modelling

105 via calibration with remotely sensed data; (2) to use the calibrated models to project climate-change

106 impacts, and (3) to assess a set of adaptation options for pastoral management identified by

107 stakeholders.

108

109 **2.   Materials and Methods**

110 *2.1. Study areas*

111   In its wide-ranging perspective, the study considered three macro-types of pastoral vegetation

112 (high, medium and low productivity) located at different altitudes (low, medium and high) in two

113 national parks of the western Alps, on either side of the French-Italian border (Stendardi et al.,

114 2022, Filippa et al., 2022) (Fig. 1).

115   Established in 1973, the *Parc National des Écrins* (PNE) covers an area of ~91800 ha

116 (approximately in the range 44° 03'-45° 05' N and 06° 05'-06° 35' E) in the two French

117 departments of Hautes-Alpes (region Provence-Alpes-Côte d'Azur) and Isère (region Auvergne-

118 Rhône-Alpes). It includes *c.* 70,000 ha of summer pastureland (~30% of the park area), which is

119 grazed by about 115,000 sheep (75% of the total stocking rate), 5,800 cows and >1,000 of goats

120 and horses. Transhumance (which is declining across Europe) is still relevant in the study area,

121   with ~1/3 of the total sheep stocking rate in summer pasture being involved in transhumance (Brien,

122   2018).

123   The *Parco Nazionale Gran Paradiso* (PNGP) is Italy's oldest national park (founded in 1922),

124   established in the core of the former Piedmontese royal hunting reserve of the alpine ibex, a species

125   of wild goat (*Capra ibex*) that lives in the mountains of the European Alps. It covers over 71,000

126   ha approximately in the range 45° 25'-45° 45' N and 07° 00'-07° 30' E in the two Italian regions

127   of Piedmont and Aosta Valley. Most of the territory (*c.* 60%) is used for non-agricultural purposes,

128   a small part (*c.*11.5%) is covered by forests, while the areas of stable grasslands are constantly

129   decreasing.

130   The surface of both parks is represented by mountainous environments, located from low valleys

131   to very high mountains, with the highest peaks of 4,102 m a.s.l. (Barre des Écrins) and 4,061 m

132   a.s.l. (Gran Paradiso Mountain) for the PNE and PNGP, respectively. The territories of the two

133   protected areas are characterised by forests, from broadleaf in the lower parts to coniferous in the

134   higher parts, and by mountain and alpine grasslands and pastures. The climate is generally alpine,

135   but with different microclimatic conditions due to high variability in topographical features

136   (elevation, aspect and slope). In addition, there are different lithological formations. All these

137   complex and variable conditions produce a large typology of different plant communities

138   characterised by a great richness of vegetation.

139

High productive pastures
Medium productive pastures
Low productive pastures

Parc National des Ècrins

Parco Nazionale del Gran Paradiso
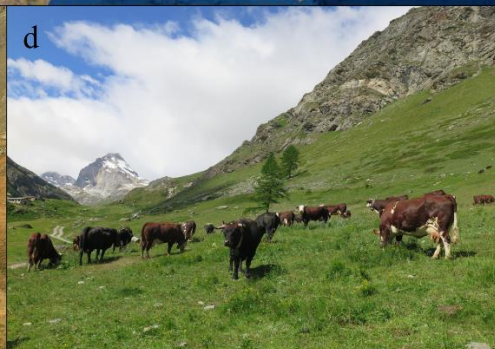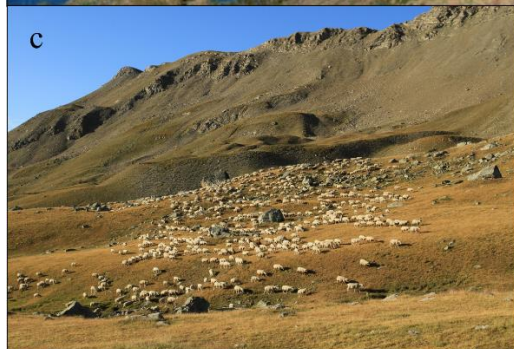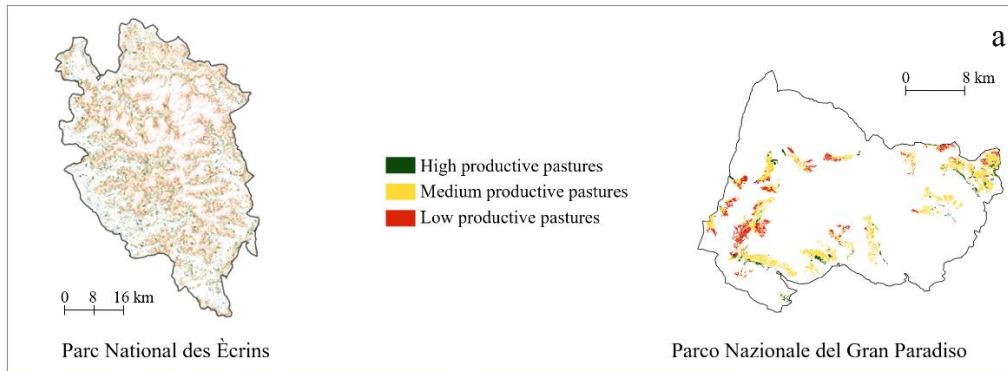
Figure 1. Location and details of the study areas: a) *Parc National des Écrins* (left) and *Parco Nazionale Gran Paradiso* (right) with localization of the high, medium and low productivity macro-types (i.e., green, yellow and red areas); b) Ikonos Panel Sharp (IPS) image from Google Earth showing Italy and the position of the two Nation parks in the alpine chain; c) example of grazing areas in the *Parc National des Écrins* and; d) in the *Parco Nazionale Gran Paradiso*.

The territories of the two parks lie within the areas of three vegetation macro-typologies (Table 1), which group the main plant communities that can be found in the subalpine and alpine pastures of the French Southern Alps (Jouglet, 1999), the Vanoise and Aosta Valley (Bornard et al., 2007) and Piedmont in Italy (Cavallero et al., 2007). These typologies have been harmonised in 13 categories of common pastures that were further grouped in three productivity macro-types (Stendardi et al., 2022).

Table 1. Description of three pastoral macro-types (HP: high productivity; MP: medium productivity; LP: low productivity) in the two study areas (PNE: *Parc National des Écrins*; PNGP: *Parco Nazionale Gran Paradiso*).

Study area	Description	Unit	Pastoral macro-types		
			HP	MP	LP
PNE	Latitude	degree N	45.04	45.06	45.06
	Longitude	degree E	06.40	06.38	06.37
	Slope	rad	0.14	0.31	0.15
	Aspect	rad	3.06	1.95	2.32
	Elevation	m a.s.l.	2044	2539	2634
	Soil depth	m	0.70	0.65	0.55
	Clay	%	30.3	34.9	27.5
	Silt	%	37.6	40.3	61.1
	Sand	%	32.1	24.8	11.4
	Soil organic carbon	g 100 g^{-1}	4.50	14.00	10.50
	Soil pH	-	5.70	5.05	4.75
	Bulk density	g cm^{-3}	0.800	0.735	0.960
	Saturated soil water content	m^3 m^{-3}	0.490	0.511	0.507
	Field capacity	m^3 m^{-3}	0.312	0.345	0.330
	Wilting point	m^3 m^{-3}	0.170	0.194	0.153

PNGP	Reference pasture type[1]	-	S6	S1	A9
	Latitude	degree N	45.56	45.57	45.58
	Longitude	degree E	07.12	07.19	07.29
	Slope	rad	0.31	0.33	0.16
	Aspect	rad	5.76	1.97	1.80
	Elevation	m a.s.l.	2133	2336	2806
	Soil depth	m	0.70	0.65	0.55
	Clay	%	6.8	6.5	6.1
	Silt	%	20.0	20.0	14.0
	Sand	%	73.2	73.5	79.9
	Soil organic carbon	g 100 g^{-1}	1.88	2.24	1.90
	Soil pH	-	5.5	4.9	5.3
	Bulk density	g cm^{-3}	1.48	1.48	1.51
	Saturated soil water content	m^3 m^{-3}	0.39	0.38	0.37
	Field capacity	m^3 m^{-3}	0.130	0.120	0.098
	Wilting point	m^3 m^{-3}	0.053	0.052	0.041
	Reference pasture type[1]	-	S-II	SA-II	A-I

[1] A-I - Alpine intermediate: sparse vegetation on medium to moderate slopes, windy ridges and bumps in the alpine level (main species: *Carex curvula*, *Trifolium alpinum*, *Avenula versicolor*); SA-II - *Nardus* swards: on lowlands and slopes in the subalpine or alpine level, vegetation of medium height (0.2-0.3 m), not very dense, dominated by *Nardus stricta* (main species: *Nardus stricta*, *Carex sempervirens*, *Trifolium alpinum*, *Festuca rubra*); A-II – nival: sparse vegetation in snow combes and moderate slopes in alpine and nival environment (main species: *Alchemilla pentaphyllea*, *Salix herbacea*, *Carex foetida*, *Plantago alpina*); S-II - subalpine intermediate: vegetation in flatlands and low slopes of the subalpine level with medium-rich soil, 0.3 to 0.5 m high, dense grassy patches dominated by fine to medium-leaved *Gramineae* (main species: *Festuca rubra*, *Agrostis capillaris*, *Phleum alpinum*, *Alchemilla xanthochlora*); S-III - *Patzkea paniculata* swards: on medium sunny slopes in the subalpine level, vegetation very tall (over 0.5 m), very dense, dominated by *Gramineae* with long, thick leaves, especially *Patzkea paniculata* (main species: *Patzkea paniculata*, *Festuca rubra*, *Carex sempervirens*).

2.2. Data collection

The Normalised Difference Vegetation Index (NDVI) is a standard way to determine vegetation cover and productivity. High NDVI values (approximately >0.7-0.8) indicate healthy vegetation, dense and productive canopies, while low NDVI values indicate land with little or no vegetation or stressed canopies. Satellite-derived NDVI data for the period 2018-2020 were retrieved for the two study areas by processing the Sentinel-2 imagery. The images (10-m spatial resolution, level2A) were atmospherically and topographically corrected with the Sen2Cor processor (https://step.esa.int/main/snap-supported-plugins/sen2cor). The images were filtered on a per-pixel basis with the scene classification (SCL) map, retaining only top quality, and cloud- and shadow-free pixels. The downloading and processing of the data were performed on Google Earth Engine (https://earthengine.google.com) with a dedicated Python (https://www.python.org) script

180   (Hufkens, 2017). Seasonal NDVI trajectories were used to retrieve growing season start and end

181   based on a fixed threshold method (20% seasonal amplitude) similar to what proposed by Shen et

182   al., (2015a). These dates were then compared to those retrieved form the snow cover seasonal

183   pattern (table 1) and found to be in good agreement. Aboveground biomass (AGB) and leaf area

184   index (LAI) were measured in both areas following standardised protocols (Filippa et al., 2015).

185   An empirical model was fitted between AGB/LAI observations and the corresponding S2-derived

186   NDVI, and the resulting equations (Supplementary material, section 1) were then used to convert

187   S2-NDVI data in AGB and LAI data for the three productivity macro-types of each study area.

188

189   *2.3.   Climate-change scenarios*

190   Simulated pastoral outputs were obtained by forcing impact models (section 2.5) with daily

191   downscaled weather data, which were selected to map a broad range of climate outcomes for impact

192   modelling (Wilcke and Bärring, 2016). Supplementary material (section 2) describes the methods

193   used in processing and post-processing the climate output used in the generation of climate

194   scenarios.

195   Climate data from three Regional Climate Models (RCMs) from Med-CORDEX (Ruti et al.,

196   2016) - CNRM-ALADIN ($0.11° \times 0.11°$), ICTP-RGCM4 ($0.44° \times 0.44°$), and CMCC-CCLM4

197   ($0.44° \times 0.44°$) for the reference period 1981-2010 (near past) and for two future time-slices 2011-

198   2040 (near future) and 2041-2070 (mid future). For near past period ambient CO_2 concentration

199   was fixed to 400 ppm. For future periods, Representative Concentration Pathways 4.5 and 8.5

200   (RCP4.5, RCP4.5) were selected, with ambient CO_2 concentration at 450 (RCP4.5) and 470 ppm

201   (RCP8.5) for near future and 540 and 670 ppm for mid future.

202   The delta-change approach was applied as a downscaling procedure, where the observed daily

203   weather data available for each given site were modified using as forcing factors the outcomes

10

204   obtained from the RCM simulations. These were calculated as the mean absolute monthly

205   differences between the RCM baseline (1981-2010) and the future RCM periods selected for

206   simulations (2041-2070, 2071-2100) for minimum and maximum air temperatures and the

207   percentage variation in monthly cumulated rainfall, wind speed and solar radiation. These

208   differences were then added, month by month, to the observed daily meteorological data from PNE

209   and PNGP to derive future weather data that were used to feed model simulations for future periods.

210   The three daily datasets deriving from RCMs downscaling were finally merged into a single dataset

211   reproducing the mean change in climate conditions for each study area in RCP4.5 and 8.5 for 2031-

212   2040, 2041-2070 and 2071-2100 time-slices.

213

214   *2.4.   Participatory approach*

215   To understand the impact of climatic events and changes in grazing practices, and to preserve

216   (or restore) the sustainable management of these areas, the "Sentinel Alpine Pastures" programme

217   focuses on how to adapt to different phenomena as part of a long-term approach to the complex

218   dynamics of climate change, to anticipate adaptive strategies (Dobremez et al., 2014). These

219   sources of information thus represent a unique opportunity to environmentally characterise these

220   pastoral areas by using advanced techniques such as remote sensing and process-based simulation

221   modelling. As a basis for the design and assessment of the analytical framework, a participatory

222   process was conducted since 2018 with groups of *c.* 100 local stakeholders in each park including

223   farmers, technicians, representatives of the two parks and officials from local institutions. The

224   participatory process involved meetings, interviews and informal discussions that took place in

225   parallel with data collection and territorial analysis (Targetti et al., 2019). Participation addressed

226   three main topics: i) current pastoral practices, related barriers and incentives, and key drivers of

227   socio-economic change; ii) effective adaptation measures already implemented in the western

11

228   Alps; and iii) which measures should be prioritised (Piccot et al., 2022). In this study, we assessed

229   the effect of prioritised adaptation options from a modelling perspective as it emerged from the

230   participatory approach, recognising the limited set of modelling assumptions contained in the

231   adaptation requests, which represent a fraction of plausible adaptations and a step towards

232   transformative changes (Holman et al., 2019).

233

234   *2.5.   Grassland modelling*

235   Process-based models are important tools in agricultural and environmental research to

236   extrapolate local observations over time and space, and to assess the impact of climate and

237   agricultural practices on the soil-plant-atmosphere continuum through plant-soil feedback effects.

238   These widely tested models are also recognised as effective tools for studying the magnitude and

239   spatial-temporal patterns of C-N (carbon-nitrogen) fluxes, playing a prominent role in testing the

240   effect of specific changes in management, plant properties or environmental factors, and in

241   designing policies specific to the soil, climate and agricultural conditions of a location or region.

242   However, the results from different models often differ, presenting a range of possible impacts and

243   adaptation responses (Brilli et al., 2017), which are influenced by the models' users' knowledge

244   and expertise, and their understanding of the variables determined in the target agroecosystems

245   (Albanito et al., 2022).

246   Here, the soil-vegetation generic model DayCent (Parton et al., 1994, 1998) and the grassland-

247   specific model PaSim (Riedo et al., 1998) were chosen to simulate alpine pastures. Both provide a

248   mechanistic view of the multiple processes and interactions occurring in grassland systems and are

249   able to simulate grassland productivity and C and N fluxes under alternative management options.

250   DayCent is the daily time-step adaptation of the biogeochemical model CENTURY (Parton et al.,

251   1994), which simulates plant growth, soil C dynamics, N leaching, gaseous emissions (e.g. nitrous

252   oxide) and C fluxes (e.g. net ecosystem exchange) in a variety of managed ecosystems. PaSim is a

253   grassland-specific ecosystem model consisting of detailed sub-models for vegetation, animals,

254   microclimate, soil biology, soil physics and management to simulate grassland productivity and C-

255   N fluxes.

256

257   *2.6.   Simulation design*

258   The modelling work was carried out in three suites of simulations: suite 1 with observational

259   data (model calibration), suite 2 with projected scenarios of climate change (impact projections),

260   and suite 3 with altered management under projected scenarios of climate change (adaptation

261   assessment).

262   Model calibration (suite 1) was carried out over the years 2018 to 2020 in the two parks, setting

263   management practices (grazing intensity and periods) as defined in Table 2 (one or two short

264   periods with short-term, intensive management), on a set of parameters (Table S1 and Table S2) to

265   which model sensitivity was determined in previous studies for both DayCent (e.g. Fitton et al.,

266   2014; Necpálová et al., 2015) and PaSim (e.g. Ben Touhami et al., 2013; Ma et al., 2015; Pulina et

267   al., 2018; Sándor et al., 2018). The agreement between simulated and observed dry matter (DM)

268   was assessed by inspection of time-series graphs (fluctuations of output variables over time), and

269   numerically, through two commonly used performance metrics of model evaluation (Richter et al.,

270   2012): root mean square error (best, g DM m^{-2} $0 \leq RMSE < +\infty$ g DM m^{-2}, worst) and coefficient of

271   determination (worst, $0 \leq R^2 \leq 1$, best).

272 Table 2. Management of three pastoral macro-types (HP: high productivity; MP: medium productivity; LP: low productivity) in the two

273 study areas (PNE: *Parc National des Écrins*; PNGP: *Parco Nazionale Gran Paradiso*). Grazing 1 and Grazing 2 refer to the first and

274 second (if present) grazing periods expressed as days of the years, respectively, over the investigated macro-types. Livestock Standard

275 Unit (LSU) refers to a dairy cow producing 3000 kg of milk per year, without additional concentrated feed (EC, 2008).

Site	Pasture macro-type	Grazing 1st						Grazing 2th					
		Period (days of year)			Stocking density (LSU ha^{-1} d^{-1})			Period (days of year)			Stocking density (LSU ha^{-1} d^{-1})		
		2018	2019	2020	2018	2019	2020	2018	2019	2020	2018	2019	2020
PNE	HP	196-197	197-198	191	120	113	126	287-288	272-273	262	43	37	76
	MP	213-214	213-214	214-215	51	49	62	-	-	-	-	-	-
	LP	217	220	217	12	10	9	-	-	-	-	-	-
PNGP	HP	194-195	198	196-197	104	98	84	261	264	264	102	106	118
	MP	229-230	230-231	229-230	79	75	57	-	-	-	-	-	-
	LP	217-218	202	222-223	30	14	20	-	-	-	-	-	-

276

277   With suite 2, we assessed the projected response of DayCent and PaSim to climate-change forcing

278   options described in section 2.3. Impacts of climate change were calculated on the changes in a set

279   of climate and ecosystem variables related to biomass production and C-N fluxes (Table 3).

280   Table 3. Climate-change impact metrics.

Type	Output	Acronym	Unit	Description
Date	Snow cover start	SCs	day of year (doy)	First of 10 consecutive days of the year with snow cover ≥5 cm
	Snow cover end	SCe		First of 10 consecutive days of the year with snow cover ≤5 cm
	Growing seasons start	GSs		First day of the year with aboveground biomass (SCe + 1 day)
	Growing seasons end	GSe		Last day of the year with aboveground biomass (SCs – 1 day)
	Biomass peak date (period 1)	BP1a		Day of the year with the highest value of aboveground biomass before the first grazing period
	Biomass peak date (period 2, HP)	BP2a		Day of the year with the highest value of aboveground biomass after the first grazing period and before the second grazing period
Count	Snow cover length	SC	days	Number of days between SCs and SCe
	Growing season length	GS		Number of days between the GSs and GSe
Amount	Biomass peak (period 1)	BP1b	kg DM m^{-2}	Aboveground biomass value at the first peak date
	Biomass peak (period 2, HP)	BP2b		Aboveground biomass value at the second peak date
	Above ground biomass	AGB	kg DM m^{-2} yr^{-1}	Annual mean aboveground biomass
	Net ecosystem exchange	NEE	kg C m^{-2} yr^{-1}	C-N fluxes
	Net primary production	NPP		
	Ecosystem respiration	RECO		
	Gross primary production	GPP		(they include emissions from ecosystem respiration (RECO = plant + soil + animal respiration), as well as estimates of the plant production of organic compounds from atmospheric CO_2 (GPP) and other system variables: NEE = RECO - GPP, NPP = GPP - plant respiration, enteric emissions of CH_4 from grazing animals and N_2O emissions from the N cycle)
	Methane	CH$_4$	kg C m^{-2} yr^{-1}	
	Nitrogen dioxide	N$_2$O	kg N m^{-2} yr^{-1}	
	Soil water content	SWC	m^3 m^{-3}	Soil water content

281

282   With the adaptation assessment (suite 3), we show the simulated outputs using the two grassland

283   models fed with the following adaptation practices, defined during the participatory process

284   (section 2.4) combined with climate-change forcing: the stocking rate in the pasture was increased

285   or decreased by 20% (LD-20% and LD+20%, respectively), and the grazing period was advanced

286   by 14 days (GDadv).

287   Simulation results are presented separately per study area, comparing DayCent and PaSim

288   outputs with satellite-derived AGB data (suite 1). Time-series graphs are presented to illustrate the

289   dynamics of selected variables (AGB, SWC, C fluxes and CH_4 and N_2O emissions) for suites 2 and

290   3, as well as two-dimensional colour data visualisations (heatmap graphs).

291

292   **3.   Results**

293   For greater clarity in the presentation of results and discussion, we present in detail only the

294   results obtained in the high productivity macro-type for which a full modelling analysis is available.

295   We also briefly present the results obtained in the medium and low productivity macro-types,

296   which are fully provided in the Supplementary material.

297

298   *3.1.   Climate analysis*

299   The monthly distribution of air temperatures in the two study areas (Fig. 2), averaged from the

300   outputs of the ICTP-REGCM4, CMCC-CCLM4 and CNRM-ALADIN climate models, showed an

301   overall increase in temperature towards the far future, similar for both parks, with a distinct

302   seasonal trend, with the highest increases in summer (+4 °C at PNE and +3.7 °C at PNGP under

303   the warmest scenario) and the lowest in autumn-winter (+2.5 °C at PNE and +2.3 °C at PNGP

304   under the warmest scenario). Analysis of simulated monthly rainfall data (Fig. 2) showed increases

305   in autumn-winter (November-February) relative to the baseline in both scenarios and sites (PNE:

306 +3.3% and +9.9%; PNGP: +5.4 % and +9.5 %, for RCP4.5 and RCP8.5, respectively), while

307 spring-summer exhibited a strong decrease in rainfall, more pronounced in the PNE (-11.7% and -

308 18.8%, for RCP4.5 and RCP8.5, respectively) than in the PNGP (-10 % in both scenarios). In both

309 parks, no clear trend was observed, nor was a clear pattern evident when analysing the differences

310 between time-slices, as there was no trend of increasing/decreasing monthly precipitation in the

311 progression from the near to the far future.
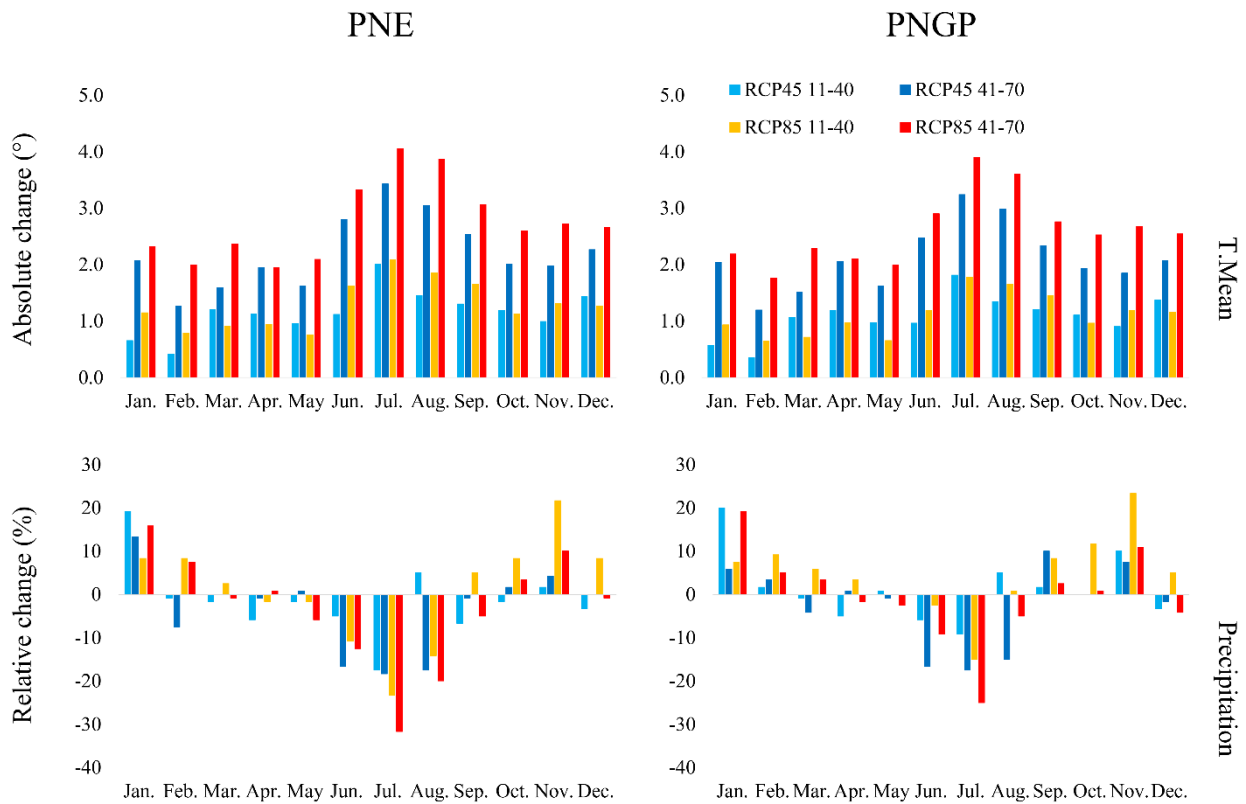
312

313 Figure 2. Absolute change (°C) in monthly mean air temperature (top graphs) and relative change

314 (%) of monthly cumulated rainfall (bottom graphs) generated in the two study areas with the RCM

315 ensemble (ICTP-REGCM4, CMCC-CCLM4 and CNRM-ALADIN) for two climate scenarios

316 (RCP4.5, RCP8.5) and two future periods - 2011-2040 and 2041-2070 - over the baseline period

317 1981-2010.

318

18

3.2.   Suite 1 of simulations: model evaluation against observed data

320   The resulting sets of parameter values allowed the outputs of the two impact models to be

321   compared for each study area. Plant parameters served to accommodate changes in the sward

322   structures driven by local environmental conditions and management. Although no formal

323   sensitivity analysis was conducted for the model parameters, the calibration applied separately to

324   each study area allowed us to explore the variability of parameter values between the two parks.

325   An indication from the calibration work is that, for both models, the parameter values can be

326   considerably different across alternative conditions (Table S1 and Table S2). For instance, the

327   different vegetation patterns in the two parks are reflected in the PaSim parameter "maximum

328   specific leaf area", whose lower values tend to be associated with the PNGP (e.g. for the high-

329   productivity pastoral vegetation macro-type, the value decreased from ~37 m^2 kg^{-1} in the PNE to

330   ~22 m^2 kg^{-1} in the PNGP). Photosynthetic rates estimated with PaSim (Table S1) were lower in the

331   PNGP during the reproductive stage (*pmco2rep*~25 µmol C m^{-2} s^{-1} against ~32 µmol C m^{-2} s^{-1} in

332   the PNE) and higher during the vegetative stage (*pmco2veg*~16 µmol C m^{-2} s^{-1} against ~13 µmol

333   C m^{-2} s^{-1} in the PNE). With DayCent, air temperature thresholds (optimal and maximum), the

334   number of soil layers influencing water and nutrient availability, and the allocation of C to different

335   plant organs influenced plant growth and C fluxes. Specifically, for the high-productivity pastoral

336   vegetation macro-type, the coefficient for calculating potential monthly aboveground biomass

337   production as a function of solar radiation outside the atmosphere lowers from 4.1 in the PNGP to

338   ~1.0 m^2 kg^{-1} in the PNE, while the thresholds for optimal air temperatures were slightly higher in

339   the PNGP than in the PNE (Table S2).

340   Standing biomass simulations (Fig. S2, Table S3) indicate that estimates substantially reflect

341   patterns of vegetation dynamics (R^2>0.50) although some departures from observed data are noted.

342   RMSE values (>70 g DM m^{-2}) are comparable with results from previous modelling studies (e.g.

343   Sándor et al., 2018), with simulations for grasslands being generally less accurate compared to

344   arable crops (e.g. Kollas et al., 2015). We also note that the great deal of fundamental research

345   incorporated into the most mechanistic PaSim model has not always improved the results.

346

347   *3.3.   Suite 2 and 3 of simulations: impacts of future scenarios and adaptation strategies*

348   For both parks, we assessed the sensitivity of the two grassland models to (suite 2) climate

349   change (RCP4.5 and RCP8.5 for the near and far future) with business-as-usual (BaU) management

350   and to (suite 3) management scenarios (GDadv and LD±20%). Multi-year mean responses for

351   selected production (AGB), biophysical (SWC) and biogeochemical (C-N fluxes) outputs are

352   presented below.

353

354   *3.4.   Growing season*

355   Under the climate-change scenarios, with both grassland models, the estimated length of the

356   snow season decreases in both areas due to earlier spring snowmelt and later autumn/winter

357   snowpack accumulation. This condition leads to an earlier onset and later end of the growing season

358   (GS) in both parks, especially in the far future (i.e. 2041-2070) (Fig. 3). Specifically, using

359   DayCent, the start of the growing season (GSs) was on average 11 and 28 days earlier in the PNE,

360   and 12 and 39 days earlier in the PNGP, for the 2011-2040 and 2041-2070. The end of the growing

361   season (GSe) was delayed on average 8 and 17 days in the PNE, and 17 days in the PNGP for 2041-

362   2070. In contrast, no changes in GSe were observed in PNGP for the period 2011-2040.

363   Using PaSim, GSs was advanced by 14 and 31 days on average in the PNE, and by 7 and 19

364   days in the PNGP for the periods 2011-2040 and 2041-2070. GSe was delayed by 5 and 23 days

365   on average for the periods 2011-2040 and 2041-2070 in the PNE, and by 36 days in the PNGP for

366   both time-slices.

367
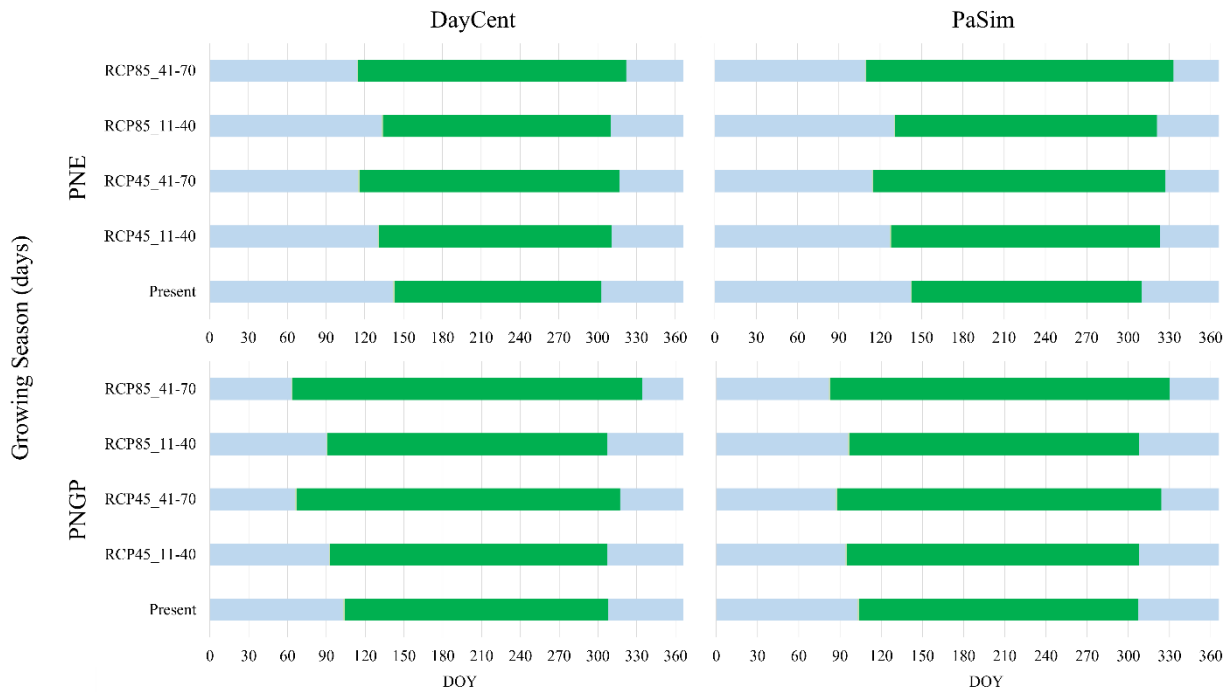
Figure 3. Estimated durations (20-year mean values) of snow-cover periods (SC, grey bars) and vegetation growing seasons (green bars) with two grassland models for baseline and climate-change scenarios under business-as-usual management in both parks for the high productivity (HP) macro-type. The annual pattern was reported at daily time-step (DOY: day of the year).

The MP and LP macro-types showed similar growing season patterns to those observed in the HP macro-type, with GSs advanced and GSe delayed towards the end of the century, with the largest impacts using RCP8.5. For all three macro-types, DayCent reported a mean GS extension ranging between 15 and 40 days in the PNE, and between 12 to 45 days in the PNGP for the periods 2011-2040 and 2041-2070, respectively. Using PaSim, the increase in GS ranged between 17 and 44 days in the PNE, and between 23 and 35 days in the PNGP for the periods 2011-2040 and 2041-2070, respectively (Fig. S3 and Fig. S4). Overall, both models suggested a longer growing season of 2 to 5 weeks when approaching the warmest scenarios.

382

383 *3.5. Soil water content (0.30 m topsoil)*

384   Under the climate-change scenarios, both models indicated an earlier decline in SWC, near or

385 below the permanent wilting point (Table 1), especially during the warm season in both parks (Fig.

386 4). PaSim showed less pronounced oscillations in SWC (~0.30-0.40 m^3 m^{-3} in the PNE and ~0.15-

387 0.25 m^3 m^{-3} in the PNGP), while DayCent interpreted the increased water supply projected by

388 climate modelling in winter (Fig. 2) to amplify seasonal differences (i.e. an excess SWC in winter

389 followed by a deficit in summer), with ~0.15-0.60 m^3 m^{-3} in the PNE and ~0.05-0.35 m^3 m^{-3} in the

390 PNGP (i.e. even below the permanent wilting point). Despite the differences between the two

391 models, for both parks the simulated patterns suggest that with drier summer conditions, grassland

392 growth may be limited by water in summer (Fig. 4).

393
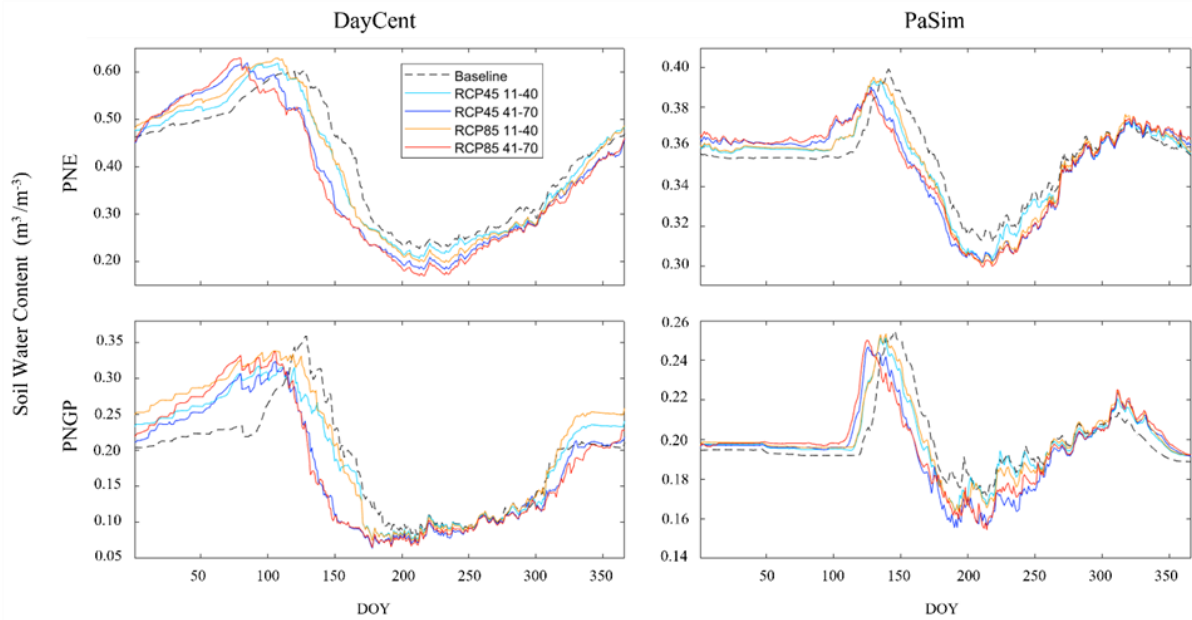
394

395 Figure 4. Simulated annual pattern (20-year mean values) of 0.30-m soil water content (SWC) with

396 two grassland models (DayCent, PaSim), for baseline and climate-change scenarios under

22

397   business-as-usual management in both parks for the high productivity (HP) macro-type. The annual

398   pattern was reported at daily time-step (DOY: day of the year).

399

400   The MP and LP macro-types showed SWC patterns similar to those observed for the HP macro-

401   type, with a reduction in SWC when approaching warmer scenarios and less pronounced SWC

402   oscillations in PaSim compared to DayCent (Fig. S5 and Fig. S6). In the MP macro-type, the SWC

403   simulated by DayCent ranged over ~0.20-0.65 m^3 m^{-3} in the PNE and ~0.05-0.40 m^3 m^{-3} in the

404   PNGP, whereas with PaSim, the SWC was in the range ~0.30-0.45 m^3 m^{-3} in the PNE and ~0.12-

405   0.24 m^3 m^{-3} in the PNGP (Fig. S5). In the LP macro-type, the SWC simulated by DayCent ranged

406   from ~0.20-0.65 m^3 m^{-3} in the PNE and ~0.05-0.40 m^3 m^{-3} in the PNGP, while with PaSim, the

407   SWC was in the range ~0.32-0.48 m^3 m^{-3} in the PNE and ~0.12-0.22 m^3 m^{-3} in the PNGP (Fig. S6).

408

409   *3.6.   Aboveground biomass*

410   Figure 5 shows the yearly average AGB production patterns under baseline management in both

411   parks for the HP macro-type as obtained with the two grassland models, while the yearly average

412   AGB patterns obtained with all alternative management options can be found in the Supplementary

413   material (Figs. S7-S10). The main differences in AGB patterns among alternative management and

414   climate scenarios were assessed based on changes in peak biomass dates (BP1a and BP2a) and

415   corresponding AGB values (BP1b and BP2b), which strongly influence stakeholders' and farmers'

416   decisions in choosing the most suitable periods for grazing.

417
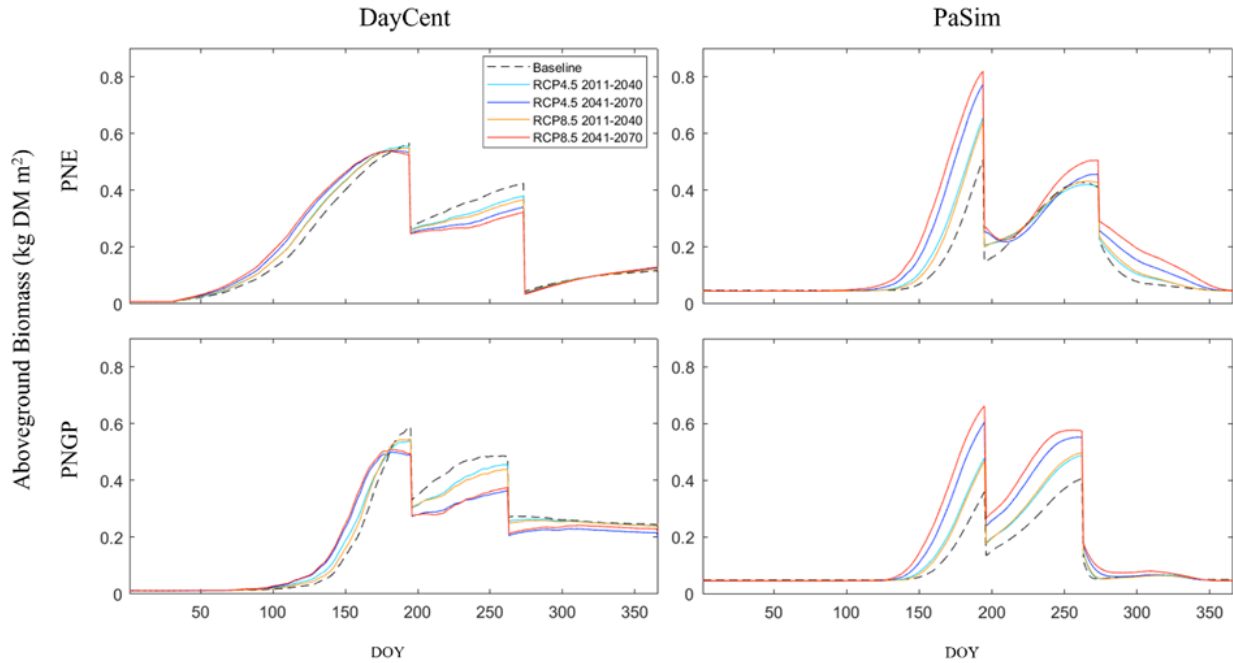
Figure 5. Simulated annual pattern (20-year mean values) of aboveground biomass (AGB) with two grassland models, for baseline and climate-change scenarios under business-as-usual management in both parks for the high productivity (HP) macro-type. The annual pattern was reported at daily time-step (DOY: day of the year).

Under the baseline climate scenarios, DayCent reported the first biomass peak (BP1a) on day 189 (±9 standard deviation) and 190 (±8 standard deviation) for the PNE and PNGP, respectively. Under future climate scenarios, the model indicated an advance of BP1a of 7-10 days for the PNE and 3-7 days for the PNGP (Table S4). In contrast, the biomass peak simulated by PaSim was mainly driven by the effect of grazing, showing only a slight advance under the future scenarios (i.e. 2-3 days) for both PNE (194±4) and PNGP (196±5, Table S5).

For the second biomass peak (BP2a), DayCent indicated that biomass peaks were at day 267 (±14 standard deviation) in the PNE and day 244 (±13 standard deviations) in the PNGP under the baseline scenarios, while future scenarios suggested advanced biomass peaks of 3 to 15 days in the

24

433   PNE and contrasting patterns (from -3 to +2 days) in the PNGP (Table S4). PaSim indicated that

434   BP2a was on day 262 ($\pm$7 standard deviation) in the PNE and on day 260 ($\pm$2 standard deviation)

435   in the PNGP under baseline scenarios, while the future scenarios indicated no or slight delay (1-5

436   days) in the PNGP and PNE, respectively (Table S5).

437   In the baseline scenarios, the biomass production of the first peak (BP1b) is similar with both

438   models in the PNE (~0.52$\pm$0.06 kg DM m^{-2}), while in the PNGP it is ~38% lower with PaSim

439   compared to DayCent (~0.61$\pm$0.17 kg DM m^{-2}). For the second peak (BP2b), the biomass value

440   provided by DayCent (0.44$\pm$0.06 kg DM m^{-2}) was close to that provided by PaSim (0.43$\pm$0.08 kg

441   DM m^{-2}) in the PNE, while at the PNGP the biomass simulated by DayCent (0.52$\pm$0.14 kg DM m^{-2}

442   ^{2}) was higher compared to that provided by PaSim (0.41$\pm$0.06 kg DM m^{-2}). Future patterns for

443   BP2b partly mirror those of BP1b, with PaSim providing an increase in biomass production of

444   ~18% in the PNE and ~41% in the PNGP as the warmer scenarios are approached, while DayCent

445   reported a decrease in biomass production of ~20% in both study areas (Table S4 and Table S5).

446   These results mainly reflect calibration against observational patterns (Fig. S2), with the PaSim

447   production profile indicating faster plant growth in spring, with a distinct peak biomass, and rapid

448   regrowth in summer. This behaviour is much more evident in the climate-change scenarios,

449   resulting in differences in AGB that are about 38-45% higher at the peak with PaSim than with

450   DayCent (Fig. 5), likely due to the absence of sensible water deficits simulated by PaSim (Fig. 4).

451   For the MP and LP macro-types (Tables S6-S9), the biomass peaks (BP1b and BP2b) partly

452   reflect the trends found in the HP macro-type. Specifically, while PaSim reported an increase in

453   peak biomass value of 50-100% with warmer scenarios in all macro-types for both parks, DayCent

454   indicated a decrease of 3-20% with the sole exception of the LP macro-type in the PNE, where

455   biomass production increased of ~25%. For the impact of adaptation strategies, the value of peak

456   biomass obtained with alternative management practices (i.e. BaU + adaptation management

457　options) was compared with the peak biomass of business-as-usual (BaU) management under

458　projected scenarios. To simplify the reading, only the first biomass peak of the HP macro-type in

459　both parks is reported here (Fig. 6), while the dynamics of the second peak (Fig. S11) and those of

460　the MP and LP macro-types are reported in the Supplementary material (Tables S6, S7, S8 and

461　S9).

462　　Using DayCent, in the PNE under RCP4.5 (blue), on average, the highest AGB values at the

463　first biomass peak compared to BaU (0.52 ± 0.06 kg DM m^{-2}) was obtained with LD+20% at both

464　current (+18.3%) and advanced (+13.5%) dates (Fig. 6). Only a slight increase was observed with

465　the other strategies (+1 to +7.7%). Under RCP8.5 (orange), BP1b shows a similar pattern to that

466　observed under RCP4.5, with higher values occurring with the adoption of the LD+20% strategy

467　at both current (+16.3%) and advanced (+13.4%) dates, and a slight mean increase using other

468　strategies (+3.8 to +6.7%). In the PNGP, under RCP4.5, a decrease in BP1b values compared to

469　current BaU (0.61 ± 0.17 kg DM m^{-2}) was observed with all alternative strategies, with the smallest

470　decrease when adopting LD+20% (-5.4%) and the highest when using GDadv_LD-20% (-18%).

471　Under RCP8.5 (Fig. 6b), BP1b showed a similar pattern and magnitude to those observed under

472　RCP4.5, with the largest decrease when adopting Gdadv_LD-20% (-17.2%) and the lowest when

473　using LD+20% (-4.9%).

474　　Using PaSim, all management options showed an increase in peak biomass under all climate

475　scenarios and time-slices. Specifically, in the PNE under RCP4.5, higher BP1b values compared

476　to BaU (0.50 ± 0.17 kg DM m^{-2}) were observed, on average, when the same grazing dates were

477　maintained with all management options (+43%) while a smaller increase was observed when

478　grazing dates were advanced (+11.7%). Under RCP8.5, BP1b shows a similar pattern to that

479　observed under RCP4.5, with higher values occurring when both current (+46%) and advanced

480　(+16.7%) grazing dates are adopted. In the PNGP, under RCP4.5, BP1b values compared to BaU

26

481   (0.37±0.11 kg DM m^{-2}) were observed, on average, both maintaining the same grazing dates with

482   all management options (+47.3%) and advancing grazing dates (+23.9%). Under RCP8.5, BP1b

483   showed the same pattern as under RCP4.5, with higher values at both current (+53.6%) and

484   advanced (+32.4%) grazing dates. Overall, DayCent showed less variability in peak biomass

485   production in the PNE than in the PNGP, with increasing variability as we approach the far future

486   (2041-2070) with the warmest scenario (i.e. RCP8.5) in both parks. In contrast, PaSim indicated

487   greater variability in peak biomass production in the PNE than in the PNGP, with decreasing

488   variability towards the far future with the warmest scenario in the PNE and contrasting patterns in

489   the PNGP.

490
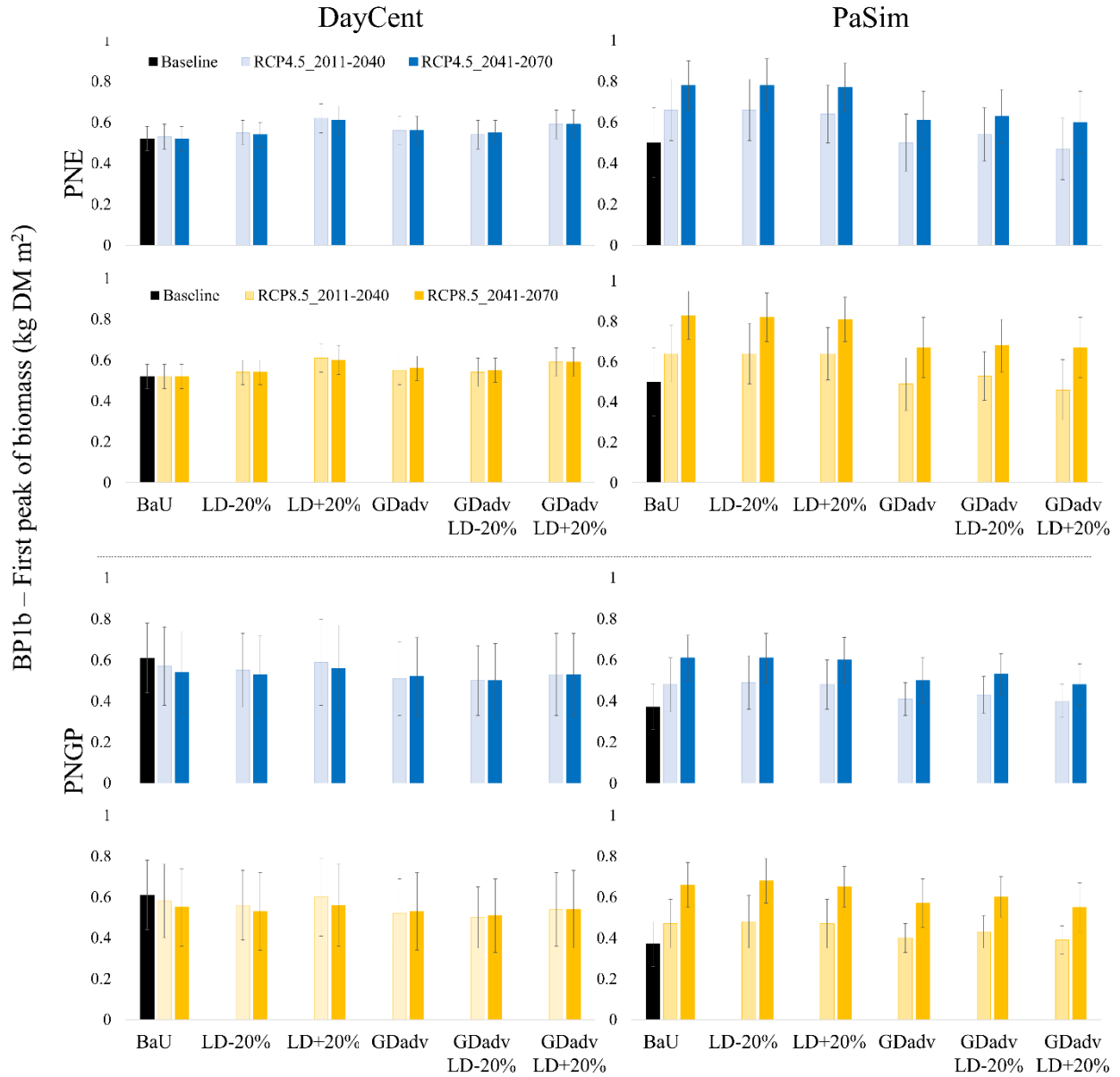
Figure 6. Changes in the first (BP1b) peak aboveground biomass (kg DM m^{-2}) between business-as-usual management (BaU) under baseline climate (black histogram) and all alternative management options under RCP4.5 (cyan and blue histograms) and RCP8.5 (clear and dark orange histograms) for high productivity pasture (HP) in both parks as provided by DayCent and PaSim. Vertical bars are standard deviations.

498   For the MP and LP macro-types, PaSim suggested a generalised increase in biomass production

499   that was particularly large (>50%) in the PNE and smaller in the PNGP across all macro-types. In

500   contrast, DayCent reported no decline or a decrease (-6%) in production for the MP macro-type in

501   both parks, regardless of advanced grazing management, while for the LP macro-type it showed

502   contrasting patterns. Specifically, a slight decrease in productivity (-4%) was observed in the PNGP

503   when approaching the warmest scenario, irrespective of management, while a 10-20% increase in

504   productivity was found in the PNE when approaching the warmest scenario at the current grazing

505   date and with different livestock densities (i.e. BaU, LD-20% and LD+20%).

506

507   *3.7.   Carbon-nitrogen fluxes*

508   Under current climate and management conditions, PaSim shows limited non-CO_2 emissions in

509   both parks, i.e. 1.9 and 1.6 g C m^{-2} yr^{-1} for CH_4 and 1 and 3 g N m^{-2} yr^{-1} for N_2O emissions, while

510   the C exchanges (NEE) vary from a limited sink in the PNE (-41 g C m^{-2} yr^{-1}) to a limited source

511   in the PNGP (+96 g C m^{-2} yr^{-1}). DayCent represents a higher sinking pattern (-350 and -308 g C m^{-}

512   ^{2} yr^{-1}) and lower CH_4 emissions (2.5E-04 and 1.2E-04 g C m^{-2} yr^{-1}) in both parks, while N_2O

513   emissions (0.5 and 3.8 g N m^{-2} yr^{-1}) are in agreement with PaSim (Table 4).

514

515   Table 4. C-N emissions (NEE: net ecosystem CO_2 exchange; CH_4: methane; N_2O: nitrous oxide)

516   from the two study areas (baseline climate), estimated (20-year mean ± standard deviation) using

517   two grassland models. The estimated components of the C budget (GPP: gross primary production;

518   NPP: net primary production; RECO: ecosystem respiration) can be found in Supplementary

519   material (Table S10).

Site	Model	NEE	CH₄	N₂O
		g C m^{-2} yr^{-1}		g N m^{-2} yr^{-1}

PNE	DayCent	-350±14	2.5E-04±~0.0	0.5±0.1
	PaSim	-41±12	1.9±0.9	1.0±0.7
PNGP	DayCent	-308±19	1.2E-04±~0.0	3.8±1.3
	PaSim	96±11	1.6±1.0	3.0±0.9

520

The absolute values of C-N fluxes (Fig. S12) indicate that both models agree in representing the magnitude of these fluxes, and the differences are explained by the inherent features of the two model structures (i.e. animal respiration, enteric fermentation). Heatmaps of the % differences between current conditions (i.e. baseline climate and BaU management) and combinations of alternative climate and management scenarios allow the impact of altered climate and management changes on gas emissions in the two parks to be assessed (Fig. 7).

For NEE, in particular, the PaSim heatmaps show overall trends towards C uptake (more negative NEE values) in both parks (red colour) by moving towards extreme climate conditions (i.e. RCP8.5 and time-frame 2041-2070), reducing livestock density and advancing grazing dates, thus reflecting the baseline AGB pattern (Fig. 5) and the inclusion in the model of an animal component explicitly representing animal respiration and enteric fermentation (Graux et al., 2011).

In contrast, DayCent reports an increase in C sourcing (more positive NEE values) of up to 30% in both parks (green colour) when extreme climate conditions are approached, which is higher when livestock density is reduced. An increase in C uptake of up to 30% was observed at both current grazing date and advanced grazing date when the livestock density is increased.

As for CH_4 emissions, the PaSim heatmap indicates that emissions are higher (~>20%) as livestock density increases. While this pattern is clearly observed in the PNE, the results in the PNGP are more contrasted, as the earlier grazing date also leads to increased CH_4 emissions, even when livestock density is reduced. Projected climate conditions do not appear to influence the pattern of emissions, which are mainly driven by management. In contrast, the CH_4 emissions

541 estimated by DayCent are conditional on climatic conditions, with the highest emission values (up

542 to ~30%) occurring towards the end of the century (i.e. in the period 2041-2070).

543 Finally, the N_2O emissions estimated by PaSim were mainly driven by the type of management

544 adopted in the two parks, where an increase in livestock density leads to higher emissions (up to

545 ~40%), while a decrease in livestock density reduces emissions to ~50%. Unlike PaSim, DayCent

546 shows contrasting patterns between the two parks. Specifically, N_2O emissions in the PNE are

547 mainly driven by management, where increasing livestock density leads to increased emissions (up

548 to ~30%), while in the PNGP, N_2O emissions are mainly driven by the climate scenarios, with the

549 highest emissions (up to ~40%) for the period 2041-2070 under both RCPs (4.5 and 8.5).

550 Under the baseline scenario, PaSim-simulated NEE for the LP macro-type showed contrasting

551 patterns. Simulated NEE in the PNE (195±193 g C m^{-2} yr^{-1}) decreased as the warmest scenarios

552 were approached (107±181 g C m^{-2} yr^{-1}), while simulated NEE in the PNGP (151±72 g C m^{-2} yr^{-1})

553 increased as the warmest scenarios were approached (163±97g C m^{-2} yr^{-1}), making both parks

554 sources of C (Fig. S14 and Fig. S15). For the MP macro-types, NEE decreased in both parks as

555 warming scenarios approached, with the PNE still being a source of C (448±388 g C m^{-2} yr^{-1}) while

556 the PNGP turned into a sink of C (-91±81 g C m^{-2} yr^{-1}) (Fig. S14 and Fig. S15). In contrast, under

557 the baseline climate scenario, DayCent- simulated NEE in both MP (-126±36 and -163±135 g C

558 m^{-2} yr^{-1}) and LP (-9±19 and -66±41 g C m^{-2} yr^{-1}) macro-types showed negative values in both parks.

559 Under the warmest scenarios, NEE tended to decrease for all macro-types in both parks, with the

560 sole exception of the LP macro-type in the PNE, where it showed a significant increase (+90%) in

561 C uptake (Fig. S13 and Fig. S14).

562 The patterns of simulated CH_4 and N_2O emissions for the LP and MP macro-types matched

563 those reported for the HP macro-type, where the estimates provided by DayCent were mainly

564 driven by climatic conditions whilst those of PaSim were mainly related to the different

565 management types (Fig. S13 and Fig. S14).

566
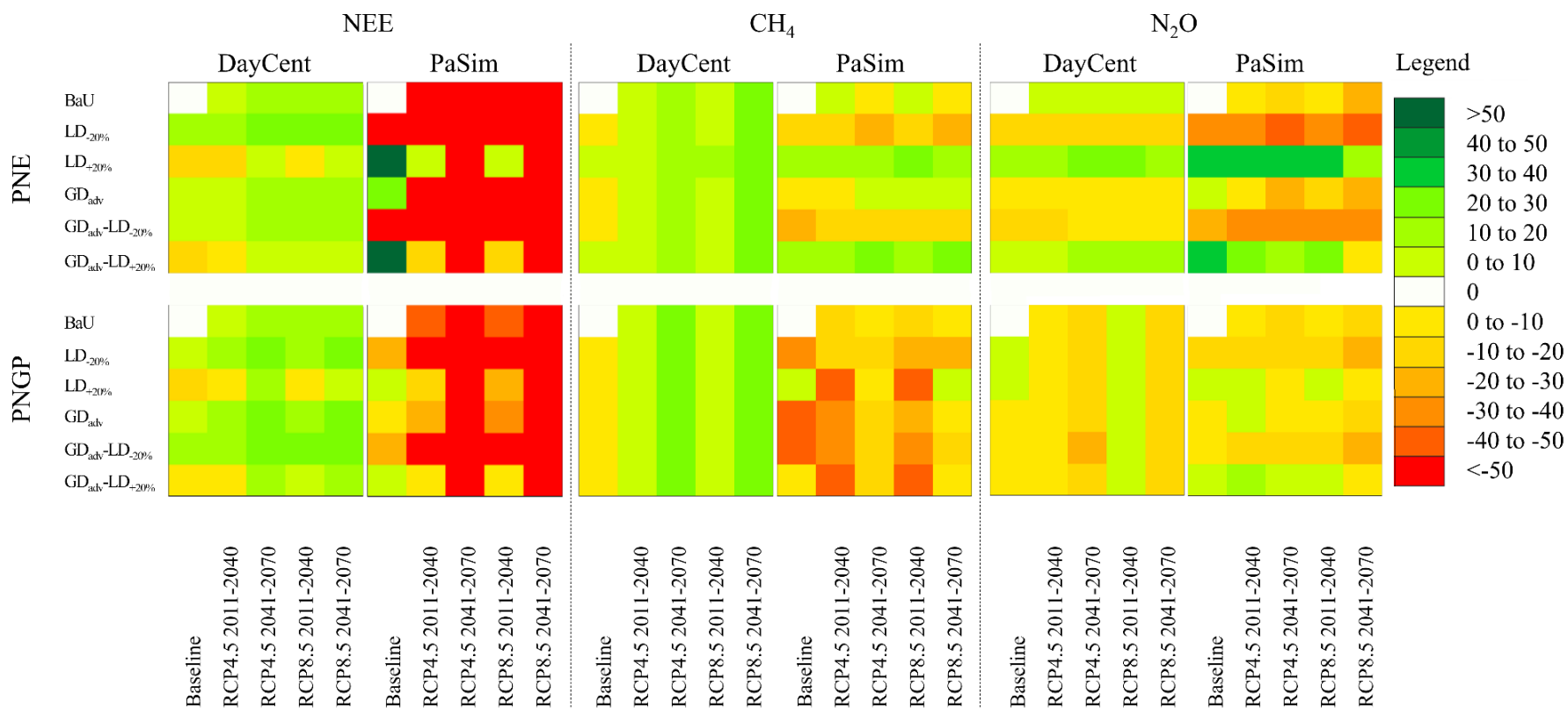
Figure 7. Heatmap visualisation of the relative differences (%) between the three main greenhouse gas emissions (NEE: net ecosystem exchange; CH_4: methane; N_2O: nitrous oxide), estimated using two grassland models (DayCent, PaSim), for alternative management and climate-change scenarios compared to the current climate and management in the *Parc National des Écrins* (PNE) and *Parco Nazionale Gran Paradiso* (PNGP). Absolute values are given in the supplementary material (Fig. S10).

571 **4.   Discussion**

572 *4.1.   Uncertainty in climate-change impact assessments*

573   The issue of uncertainty in model outputs remains a real challenge for the implementation of a

574 modelling framework in decision-making or information processes. Uncertainty can arise from

575 several sources (model structure, parameterisation, input data, initialisation), and the way it

576 manifests itself in model estimates can be difficult to determine and requires interpretation by

577 stakeholders. In this study on climate-change and impact projections in alpine pasturelands, there

578 are different levels of uncertainty on multiple elements (e.g. biophysical, socio-economic). The

579 lack of certainty about the future is primarily related to prospective views at various scales: global

580 (socio-economic scenarios), regional (land and soil use) and field (pastoral systems and

581 management). In addition, the chaotic character of the climate system, with its interannual

582 variability, limits the reliability of climate projections. For instance, the CNRM-ALADIN RCM

583 used to derive forcing factors for downscaling in the alpine context (Rousselot et al., 2012) is

584 considered relevant for high temporal frequency climate studies in the Euro-Mediterranean region

585 (Nabat et al., 2020), but substantial improvement in simulating spatial patterns and annual cycles

586 can be achieved with an ensemble of RCMs (Fantini et al., 2018). In our study, the use of ensemble-

587 mean results to estimate mean trends for alternative RCMs does not take into account the variability

588 associated with different RCMs, which respond differently to the same emission scenarios

589 (Supplementary material, section 3), and represents a simplification in the modelling design.

590   Also in the case of vegetation response to CO_2 enrichment, there are large uncertainties in the

591 (complex) climate model projections and underlying scenarios. The extent of our imperfect

592 knowledge of the processes (and their interactions) embedded in models (epistemic uncertainties)

593 is reflected in climate modelling, where it mainly concerns atmospheric and biosphere physics,

594 ocean-atmosphere coupling, embedded empirical relationships, parameterisation and spatial

34

595   resolution. At smaller scales, impact models (such as the grassland models used here) may suffer

596   from the omission or lack of consideration of long-term climate-related processes (e.g. plant

597   acclimation; Sándor et al., 2018) and their interactions (model structure), as well as changes in

598   parameter values due to new climate conditions (which may require re-parameterisation of the

599   model, e.g. Ben Touhami et al., 2015). Estimates of future conditions should be presented for

600   review by stakeholders, who can then assess the different levels of uncertainty in the multiple

601   elements and estimate their own relevant projections based on their own area of expertise. In

602   climate-change impact studies, a range of emission scenarios are used to feed climate models and,

603   in turn, impact models. Uncertainty accumulates and propagates throughout the process of climate-

604   change projection and impact assessment, which is carried out by developing fine-scale climate

605   data from coarse-scale climate models and feeding the resulting local-scale scenarios into impact

606   models to determine impacts and assess possible adaptations (Bellocchi et al., 2015). Emission

607   scenarios are neither forecasts nor policy recommendations (Moss et al., 2010) but are selected to

608   map a broad range of climate outcomes for further research and assessment, including impact-

609   modelling studies. In particular, policies contrary to those established to discuss extreme situations

610   (Cao et al., 2022) should not lead to a misuse of RCP8.5 as a no-climate-policy baseline (Pilke and

611   Ritchie, 2021).

612   Our work demonstrates the value gained by conducting a process to assess the ability of a

613   modelling framework and remotely sensed products to represent past (observational) and future

614   (projected) conditions (two-time frames), based on the outputs of two climate scenarios (radiative

615   forcing), three climate models (climate forcing) and two grassland models (impacts and

616   adaptations). For the latter, the study identified grassland models sufficiently contrasted in their

617   ability to represent processes controlling the dynamics of energy, water and C-N cycles. This

618   choice was made in order to better assess changes in model estimates as a result of changing

619 assumptions and to identify the most significant ones that reflect reality. In addition, this approach

620 helps to identify the range of variability over which model outputs may vary. In the selection phase,

621 two models were identified in which processes are represented at different levels of detail. While

622 PaSim is a complex (grassland-specific) model, simulating C-N and water cycles in detail (with a

623 module dedicated to livestock impact and livestock-atmosphere feedbacks), DayCent is a more

624 empirical (generic) model, with relatively simple relationships between driving variables and

625 fluxes. The two models differ in the representation of soil properties, vegetation type, agricultural

626 practices and environmental forcing, as well as in the initialisation of C pools. The common feature

627 of both models is that they were both designed to be applied considering the grassland community

628 as a crop with parameters describing the morphological and physiological characteristics of the

629 vegetation set at values that should represent the mean traits of the community. Consequently, their

630 ability to characterise interactions in multi-species grasslands is limited, beyond simple mixtures

631 of legumes and grasses (Van Oijen et al., 2020).

632

633 *4.2.   Analysis of climate-change impacts and adaptation strategies*

634   The two impact models adopted agreed in the representation of impacts such as the timing and

635 extent of the growing season and C-N fluxes, whilst divergences were observed for other outputs

636 (e.g. biomass production and peak production). The longer growing season simulated by both

637 models was mainly driven by the extension of the potential growing season in spring, whilst it was

638 limited during autumn-winter, reflecting long-term observations in large alpine regions

639 (Barichivich et al., 2013; Ernakovich et. al., 2014; Chen and Yang, 2020). The agreement in the

640 GS outputs suggests the ability of the models to reproduce the changing seasonality of

641 photosynthesis in vegetation, including the beginning and end of the growing season. Although

642 both models were widely applied in various contexts (e.g. Calanca et al., 2007; Abdalla et al., 2010;

643   Vital et al., 2013; Ma et al., 2015; Ben Touhami and Bellocchi, 2015; Pulina et al., 2018; Fitton et

644   al., 2019; Fucks et al., 2019, 2020; Melo-Damian et al., 2021), this is one of the few studies

645   reproducing the dynamics in alpine pastoral environments, whose multifaceted structure of territory

646   and vegetation coupled with extreme weather conditions is difficult to parameterise due to limited

647   ground-based data for initialisation, calibration and assessment, the complex response of the

648   vegetation growth and information on critical thresholds (e.g. air temperatures, water needs,

649   radiation use efficiency) for mixed plant communities. As evidence of this, the mean plant growth

650   trend simulated with both models (20-year means, Fig. 5) does not seem to reflect the observed

651   pattern of very slow or no growth during the snow season, followed by a rapid increase in biomass

652   accumulation as the snow melts. Generally, after the onset of growth in May or early June, plants

653   grow rapidly, and daily dry matter accumulation can reach a maximum within a few weeks.

654   Grassland models in their current state are not designed to properly represent such a progression

655   of biomass accumulation with the rapid attainment of the first biomass peak. If this behaviour was

656   roughly captured with the calibration work (over three years of AGB data; Fig. S2), and

657   discrepancies appeared less evident with PaSim. Also, the lack of overlap between snow-cover

658   periods and vegetation growing seasons was due to limitations inherent to the modelling of

659   complex ecosystems. Specifically, biogeochemical models are often unable to discriminate the

660   presence of snow and biomass at the same time on a given surface unit, but instead work separately

661   on it. Thus, to avoid speculation on the residual amount of snow cover and, therefore, period

662   overlap, the two components were showed separately. Considering that biophysical data show a

663   large degree of variability, and that discrepancies between model estimates and actual data are

664   common despite calibration efforts, research avenues can be opened from this assessment to

665   improve simulation models for such harsh environments as high altitude mountains, where snow

666   beds melt late and plants grow rapidly, but the rapid growth period is short during the middle of

667   the growing season, and this pattern evolves with changing climate (e.g. Wang et al., 2020). The

668   extension of data series is indeed critical, as while calibrated models provide an adequate

669   description of the available data, they may not capture known trends over long time horizons

670   (Bellocchi et al., 2010).

671   Regarding C-N fluxes, the two grassland models agreed to some extent across study areas and

672   pasture macro-types, with differences in magnitude and patterns likely associated with the inherent

673   structure of each specific C and N sub-model (e.g. Cavalli et al., 2019). The higher C uptake

674   estimated by DayCent compared to PaSim (Figs. S12, S13 and S14) reflects the fact that PaSim

675   estimates the animal contribution to ecosystem respiration, which is not accounted for in DayCent's

676   C budget. Similarly, DayCent estimated limited CH_4 emissions since (unlike PaSim) it does not

677   account for fermentative digestion in its C-N sub-model. The magnitude of N_2O emissions was

678   instead similar between the two models for each study area and macro-type. Overall, the analysis

679   also revealed that GHG dynamics were mainly driven by weather variables in DayCent and by

680   livestock management in PaSim. In this way, PaSim estimates of CH_4, and CO_2 emissions may

681   better reflect observational studies that underpin the impact of management on the annual C cycle

682   of grassland systems (as well as cropping systems), in addition to the variability of local

683   environmental drivers (Pinares-Patiño et al., 2007; Ceschia et al., 2010; Zeeman et al., 2010, 2019).

684   In particular, the importance of quantifying direct CO_2 emissions from grazing animals is

685   emphasised (e.g. Pinares-Patiño et al., 2007). In the absence of observational data to compare with

686   the simulation results, we refer to the literature on the C sequestration capacity of grasslands, which

687   reports contrasting results similar to those of Table 4, which do not exclude that mountain

688   grasslands may oscillate between being sinks and moderate sources (e.g. Zeeman et al., 2010).

689   Although the two grassland models generally agree in their impact projections, they often differ

690   in essential details, for instance with regard to future peak pasture production. Among the reasons

691   for these different results is the uncertainty inherent in the structure of the models, as well as

692   uncertainty in their parameterisation (and the generalisation of the resulting sets of parameter

693   values to broad regional studies), which in turn makes the projections themselves uncertain. When

694   considering the influence of these uncertainties on the interpretation and understanding of the

695   projections, but also on the direction of the research, it is of great value to know the factors behind

696   these uncertainties (Dietze et al., 2018). DayCent and PaSim showed different responsiveness to

697   water-related factors. The water-limited growth of DayCent rather hinders biomass growth, which,

698   according to climate scenarios, peaks before the start of grazing. With DayCent, the projected

699   scenarios indicate that the water deficit could be the limiting factor for summer growth, which

700   could be lower than in the near-past climate baseline. Consequently, DayCent projections towards

701   a greater C sourcing in the PNE are logically associated with water stress and water-limited biomass

702   production estimated by this model under future scenarios (Fig. 7), which limits photosynthetically

703   assimilated C (gross primary production). This condition requires further study of the uncertainty

704   associated with the model processes. Thus, the mean responses of alpine pasture production (and

705   related outputs) to climate change, obtained with two impact models, should be considered as two

706   extreme situations with respect to plausible future realisations: without water stress (liberal PaSim

707   approach) and with water stress (conservative DayCent approach).

708   However, there may also be biases in the simulation of SWC, with grassland models that may

709   not be accurate enough to estimate these dynamics. This is often associated with an unrealistically

710   low amplitude of the annual cycle (fluctuation damping, after Wu et al., 2002) of the soil water

711   content curve compared to field measurements (Sándor et al., 2017). It is known that the quality of

712   soil water content simulations can seriously affect model outputs. In case of poor estimation of soil

713   water content, model calibration may result in biased parameter values. Several factors, such as

714   permanent wilting point, root distribution and maximum transpiration rate, are in fact related to the

715   rate of water infiltration into the soil during precipitation events and snowmelt periods (Philip,

716   1993), which would require detailed datasets for an accurate description. Because of the known

717   role of soil water content in determining evapotranspiration rates, stomatal conductance and other

718   processes, this issue has obvious implications for sites and seasons where water shortage is a typical

719   feature. The response of the models to water-limited conditions is thus questionable, which means

720   that the applicability of the models in semi-arid or arid pastoral systems may not always be

721   supported. This is to some extent related to the ability of roots to extract water from the soil (Volaire

722   and Lelièvre, 2001). The usefulness of soil water content estimation is not as straightforward as for

723   other variables and it is clear the development of improved models is fundamentally necessary for

724   soil hydrology, to rectify structural errors in models and to avoid systematic errors associated with

725   some of the model parameters. These may involve further study of runoff, diffusion and percolation

726   processes, while accounting for features such as ponding water formation, and snowmelt and

727   groundwater movement (Hidy et al., 2016).

728

729   *4.3.   Effect of adaptation measures*

730   The climate-change scenarios exhibited an increase in the air temperature together with higher

731   winter precipitation and prolonged drier conditions during the spring-summer period. This

732   condition logically translates into an accentuation of seasonality, with faster snowmelt and a longer

733   growing season (i.e. +15 to +40 days), providing higher estimated yields and evapotranspiration in

734   both study areas. In this perspective, earlier grazing dates and changes in livestock density, which

735   were *a priori* hypothesised as adaptation options, proved to be coherent to cope with these projected

736   changes.

737   The earlier grazing date better matched the future biomass peaks simulated by DayCent, also

738   agreeing with observations in alpine regions (i.e. Xu et al., 2016) and thus resulting in a more

40

739 efficient use of pastures. Although this pattern paved the way for increasing the number of grazing

740 events during the growing season, reduced biomass regrowth due to dry summer conditions

741 inhibited the possibility of further grazing. Reduced soil water availability and increased number

742 of days of heat stress can lead to stomatal closure and inhibit biomass production in summer, which

743 must be taken into account in addition to the increase in plant photosynthetic rates with increasing

744 CO_2 concentration in the atmosphere, not to mention the possible degradation of grasslands due to

745 severe summer drought episodes (Moreau and Lorgeou, 2007). For that, any excess water in winter

746 can be used to reduce the water deficit when the soil is drier than the field capacity. While this

747 would hint at the possibility of using irrigation even at high altitudes to extend the number of

748 grazing events, the balance between costs (e.g. of energy and irrigation systems) and benefits (e.g.

749 increased end product) would need to be thoroughly investigated. In contrast, in the scenario

750 depicted by PaSim, which would be too liberal in the sense that it simulates optimal growing

751 conditions in midsummer (i.e. without an expectation of summer water stress), this adaptation

752 strategy would not be necessary.

753 The model results indicate higher biomass production when LD is increased (although changes

754 in livestock density do not particularly modify production levels). This result is likely due to a

755 higher N availability to plants provided by a higher amount of N excreted in faeces and urine which,

756 together with a simulated non-linear effect of grazing on production, led to a faster and higher

757 biomass regrowth rate. While both models consider N from excretion and the effect of grazing on

758 production, detrimental effects on biomass production due to the impact of soil compaction when

759 animal density increases were not considered. However, higher animal numbers may increase soil

760 compaction, resulting in poor water retention and altered (slower) mineralisation processes that

761 may reduce biomass regrowth and forage quality (Li et al., 2017). In this perspective, the response

762 of biomass growth to changes in LD could be partly overestimated or affected by a certain level of

763   uncertainty in both models. Despite these limitations, we can conclude that the alpine region is set

764   to become warmer and wetter, and that yields in these areas are highly dependent on both water

765   availability and the type of management adopted. The projected climate scenarios and adaptation

766   options considered are not expected to substantially worsen the GHG balance, although a caveat is

767   that C sequestration by pasturelands may be reduced in a warmer climate. However, there is a need

768   to further develop and evaluate grassland models for key processes and outputs, such as CO_2 and

769   non-CO_2 emissions, as well as to systematically and more accurately characterise the extent and

770   timing of human intervention in a range of grazing areas covering broader climatic gradients.

771

772   **5.   Concluding remarks**

773   Research on mountain pastures in two western alpine parks shows that variations in climate-

774   change impacts and adaptations of these systems are linked to natural and anthropogenic factors to

775   different degrees depending on the pastoral macro-type class studied (defined by an altitudinal

776   productivity gradient). While the use of modelling approaches and remote-sensing products in

777   vulnerability studies is not new *per se*, the integration of these tools within alpine pastoral

778   communities has a point of originality, as the analysis carried out can help to solve

779   multidisciplinary challenges such as which areas are vulnerable and how they compare under harsh

780   climatic conditions. The findings of this study indicate an increase in the length of the growing

781   season by 15 to 40 days, leading to expected changes in the timing and amount of biomass

782   production and a likely decrease in biomass regrowth during the summer season due to prolonged

783   drought conditions. The greatest uncertainties were found in the GHG balance and mitigation

784   capacity of alpine pastures, where contrasting patterns were observed between the impact models

785   used (ranging from -350 to +100 g C m^{-2} yr^{-1} for NEE), mainly due to the different flux simulation

786   approaches. Similarly, earlier grazing dates appeared to be the most suitable adaptation strategy,

787   especially when combined with increasing livestock density, while decreasing livestock density

788   did not show any significant change.

789   The elaboration of adaptation measures, carried out in this study with local herding and farming

790   communities, provides a basis for appropriate agricultural policy and land management measures

791   adapted to ongoing climate change. However, although different modelling approaches are able to

792   capture distinct aspects of the adaptive process, they tend to be applied in relative isolation, without

793   producing unified representations. The corollary of this is that the usefulness of future projections

794   of climate-change impacts by grassland models, such as those represented here, is strongly

795   influenced by the quality of the climate model data used to run them and the field data used to

796   calibrate them. Social impact assessment studies are now needed to examine how

797   production/biophysical/biogeochemical impacts, i.e. the effects of climatic anomalies on alpine

798   pasture performances, propagate through the socio-economic and political system. Such an

799   integrated approach, which would include the potential for adaptation and adjustment to climate

800   pressure, would reflect the reality of pastoral communities much better than the modelling used

801   and raises fruitful research questions on the vulnerability of alpine territories and their adaptive

802   capacity.

803

43

References

817 **References**

818 Abdalla, M., Jones, M., Yeluripati, J., Smith, P., Burke, J., Williams, M., 2010. Testing DayCent

819 and DNDC model simulations of N_2O fluxes and assessing the impacts of climate change on the

820 gas flux and biomass production from a humid pasture. Atmos. Environ. 44, 2961–2970.

821 https://doi.org/10.1016/j.atmosenv.2010.05.018

822 Albanito, F., McBey, D., Harrison, M., Smith, P., Ehrhardt, F., Bhatia, A., Bellocchi, G., Brilli, L.,

823 Carozzi, M., Christie, K., Doltra, J., Dorich, C., Doro, L., Grace, P., Grant, B., Léonard, J.,

824 Liebig, M., Ludemann, C., Martin, R., Meier, E., Meyer, R., De Antoni Migliorati, M.,

825 Myrgiotis, V., Recous, S., Sándor, R., Snow, V., Soussana, J.F., Smith, W.N., Fitton, F., 2022.

826 How Modelers Model: the Overlooked Social and Human Dimensions in Model

827 Intercomparison Studies. Environmental Science & Technology 2022 56 (18), 13485-13498.

828 https://doi.org/10.1021/acs.est.2c02023

829 Alessa, L., Kliskey, A., Gosz, J., Griffith, D., & Ziegler, A., 2018. MtnSEON and social–ecological

830 systems science in complex mountain landscapes. Frontiers in Ecology and the Environment,

831 16(S1), S4-S10. https://doi.org/10.1002/fee.1753

832 Altaweel, M., Virapongse, A., Griffith, D., Alessa, L., & Kliskey, A., 2015. A typology for

833 complex social-ecological systems in mountain communities. Sustainability: Science, Practice

834 and Policy, 11(2), 1-13. https://doi.org/10.1080/15487733.2015.11908142

835 Ayar, P.V., Vrac, M., Bastin, S., Carreau, J., Déqué, M., Gallardo, C., 2016. Intercomparison of

836 statistical and dynamical downscaling models under the EURO-and MED-CORDEX initiative

837 framework: present climate evaluations. Climate Dynamics 46, 1301-1329.

838 https://doi.org/10.1007/s00382-015-2647-5

839 Barichivich, J., Briffa, K.R., Myneni, R.B., Osborn, T.J., Melvin, T.M., Ciais, P., Piao, S., Tucker,

840 C., 2013. Large-scale variations in the vegetation growing season and annual cycle of

45

841   atmospheric CO_2 at high northern latitudes from 1950 to 2011. Global Change Biology 19,

842   3167-3183. https://doi.org/10.1111/gcb.12283

843   Bellocchi, G., Rivington, M., Donatelli, M., Matthews, K., 2010. Validation of biophysical models:

844   issues and methodologies. A review. Agronomy for Sustainable Development 30, 109-130.

845   Bellocchi, G., Rivington, M., Matthews, K., Acutis, M., 2015. Deliberative processes for

846   comprehensive evaluation of agroecological models. A review. Agronomy for Sustainable

847   Development 35, 589-605. https://doi.org/10.1051/agro/2009001

848   Ben Touhami, H., Bellocchi, G., 2015. Bayesian calibration of the Pasture Simulation model

849   (PaSim) to simulate European grasslands under water stress. Ecological Informatics 30, 356-

850   364. https://doi.org/10.1016/j.ecoinf.2015.09.009

851   Ben Touhami, H., Lardy, R., Barra, V., Bellocchi, G., 2013. Screening parameters in the Pasture

852   Simulation model using the Morris method. Ecological Modelling 266, 42-57.

853   Bengtsson, J., Bullock, J.M., Egoh, B., Everson, C., Everson, T., O'Connor, T., O'Farrell, P.J.,

854   Smith, H.G., Lindborg, R., 2019. Grasslands - more important for ecosystem services than you

855   might think. Ecosphere 10, e02582. https://doi.org/10.1002/ecs2.2582

856   Bonet, R., Arnaud, F., Bodin, X., Bouche, M., Boulangeat, I., Bourdeau, P., Bouvier, M., Cavalli,

857   L., Choler, P., Delestrade, A., Dentant, C., Dumas, D., Fouinat, L., Gardent, M., Lavergne, S.,

858   Lavorel, S., Naffrechoux, E., Nellier, Y., Perga, M.-E., Sagot, C., Senn, O., Thibert, E., Thuiller,

859   W., 2016. Indicators of climate: Ecrins National Park participates in long-term monitoring to

860   help determine the effects of climate change. Journal on Protected Mountain Areas Research

861   and Management S. 44-52. https://doi.org/10.1553/eco.mont-8-1s3

862   Bornard A., Bassignana M., Bernard-Brunet C., Labonne S., Cozic Ph., 2007. Les végétations

863   d'alpage de la Vanoise. Description agro-écologique et gestion pastorale. Éd. Quae, Versailles.

864   (in French)

46

865 Brien, P., 2018. Analyse de l'évolution de l'utilisation des alpages sur le territoire du Parc National

866   des Écrins (1996-2012), perceptions des tendances en cours et des enjeux à venir. L'exemple de

867   la prédation et du changement climatique en alpage. Rapport de stage en entreprise, Université

868   Savoie-Mont Blanc. (in French)

869 Brilli, L., Bechini, L., Bindi, M., Carozzi, M., Cavalli, D., Conant, R., Dorich, C.D., Doro, L.,

870   Ehrhardt, F., Farina, R., Ferrise, R., Fitton, N., Francaviglia, R., Grace, P., Iocola, I., Klumpp,

871   K., Léonard, J., Martin, R., Massad, R.S., Recous, S., Seddaiu, G., Sharp, J., Smith, P., Smith,

872   W.N., Soussana, J.-F., Bellocchi, G., 2017. Review and analysis of strengths and weaknesses of

873   agro-ecosystem models for simulating C and N fluxes. Sci. Total Environ. 598, 445-470.

874   https://doi.org/10.1016/j.scitotenv.2017.03.208

875 Caballero, R., Fernández-González, F., Pérez Badia, R., Molle, G., Roggero, P.P., Bagella, S.,

876   D'Ottavio, P., Papanastasis, V.P., Fotiadis, G., Sidiropoulou, A., Ispikoudis, I., 2009. Grazing

877   systems and biodiversity in Mediterranean areas: Spain, Italy and Greece. Pastos 39, 9-152.

878 Calanca, P., 2007. Climate change and drought occurrence in the Alpine region: How severe are

879   becoming the extremes? Global and Planetary Change 57, 151-160.

880   https://doi.org/10.1016/j.gloplacha.2006.11.001

881 Calanca, P., Vuichard, N., Campbell, C., Viovy, N., Cozic, A., Fuhrer, J., Soussana, J.F., 2007.

882   Simulating the fluxes of CO_2 and N_2O in European grasslands with the Pasture Simulation

883   Model (PaSim). Agriculture, Ecosystems & Environment 121, 164–174.

884   https://doi.org/10.1016/j.agee.2006.12.010

885 Cao, W., Duan, C., Yang, T., Wang, S., 2022. Higher Heat Stress Increases the Negative Impact

886   on Rice Production in South China: A New Perspective on Agricultural Weather Index

887   Insurance. Atmosphere, *13*, 1768. https://doi.org/10.3390/atmos13111768

888 Cavallero A., Aceto P., Gorlier A., Lombardi G., Lonati M., Martinasso B., Tagliatori C., 2007. I

889   tipi pastorali delle Alpi piemontesi. A. Perdisa Editore, Bologna. pp XII-467 p., ill. ,

890   EAN:9788883723216

891 Cavalli, D., Bellocchi, G., Corti, M., Marino Gallina, P., Bechini, L., 2019. Sensitivity analysis of

892   C and N modules in biogeochemical crop and grassland models following manure addition to

893   soil. Eur. J. Soil Sci. 70, 833-846. https://doi.org/10.1111/ejss.12793

894 Ceschia, E., Béziat, P., Dejoux, J.F., Aubinet, M., Bernhofer, Ch., Bodson, B., Buchmann, N.,

895   Carrara, A., Cellier, P., Di Tommasi, P., Elbers, J.A., Eugster, W., Grünwald, T., Jacobs, C.M.J.,

896   Jans, W.W.P., Jones, M., Kutsch, W., Lanigan, G., Magliulo, E., Marloie, O., Moors, E.J.,

897   Moureaux, C., Olioso, A., Osborne, B., Sanz, M.J., Saunders, M., 2010. Management effects on

898   net ecosystem carbon and GHG budgets at European crop sites. Agriculture, Ecosystems and

899   Environment 139, 363–383. https://doi.org/10.1016/j.agee.2010.09.020

900 Chen, X., Yang, Y., 2020. Observed earlier start of the growing season from middle to high

901   latitudes across the Northern Hemisphere snow-covered landmass for the period 2001–2014.

902   Environ. Res. Lett. 15: 034042. https://doi.org/10.1088/1748-9326/ab6d39

903 Chow, L., Xing, Z., Rees, H.W., Meng, F., Monteith, J., Stevens, L., 2009. Field performance of

904   nine soil water content sensors on a sandy loam soil in New Brunswick, Maritime Region,

905   Canada. Sensors 9, 9398-9413. https://doi.org/10.3390/s9110939

906 Corona-Lozada, M.C., Morin, S., Choler, P., 2019. Drought offsets the positive effect of summer

907   heat waves on the canopy greenness of mountain grasslands. Agricultural and Forest

908   Meteorology. https://doi.org/10.1016/j.agrformet.2019.107617

909 Della-Vedova M., Legeard J.P., 2012. Alpages sentinelles dans le Parc national des Écrins : un

910   espace de dialogue pour anticiper l'impact des aléas climatiques. Assemblée Générale du

911   Cerpam, La Chapelle-en-Valgaudemar (05), 18 septembre 2012. (in French)

912 Dibari, C., Bindi, M., Moriondo, M., Staglianò, N., Targetti, S., Argenti, G., 2016. Spatial data

913 integration for the environmental characterization of pasture macrotypes in the Italian Alps.

914 Grass and Forage Science 71, 219-234. https://doi.org/10.1111/gfs.12168

915 Dibari, C., Costafreda-Aumedes, S., Argenti, G., Bindi, M., Carotenuto, F., Moriondo, M.,

916 Padovan, G., Pardini, A., Staglianò, N., Vagnoli, C., Brilli, L., 2020. Expected changes to Alpine

917 pastures in extent and composition under future climate conditions. Agronomy 10: 926.

918 https://doi.org/10.3390/agronomy10070926

919 Dibari, C., Pulina, A., Argenti, G., Aglietti, C., Bindi, M., Moriondo, M., Mula, L., Pasqui, M.,

920 Seddaiu, G., Roggero, P.P., 2021. Climate change impacts on the Alpine, Continental and

921 Mediterranean grassland systems of Italy: A review. Italian Journal of Agronomy, 16:1843.

922 https://doi.org/10.4081/ija.2021.1843

923 Dietze, M.C., Fox, A., Beck-Johnson, L.M., Betancourt, J.L., Hooten, M B., Jarnevich, C.S., Keitt,

924 T.H., Kenney, M.A., Laney, C.M., Larsen, L.G., Loescher, H.W., Lunch, C.K., Pijanowski,

925 B.C., Randerson, J.T., Read, E.K., Tredennick, A.T., Vargas, R., Weathers, K.C., White, E.P.,

926 2018. Iterative near-term ecological forecasting: Needs, opportunities, and challenges.

927 Proceedings of the National Academy of Sciences of the United States of America 115, 1424-

928 1432. https://doi.org/10.1073/pnas.1710231115

929 Dumont, B, Farruggia, A, Garel, J.-P., Bachelard, P., Boitier, E., Frain, M., 2009. How does grazing

930 intensity influence the diversity of plants and insects in a species-rich upland grassland on basalt

931 soils? Grass and Forage Science 64, 92–105. https://doi.org/10.1111/j.1365-2494.2008.00674.x

932 EC, 2008. Regulation (EC) No 1166/2008 of the European Parliament and of the Council of 19

933 November 2008 on farm structure surveys and the survey on agricultural production methods

934 and repealing Council Regulation (EEC). Official Journal of the European Union, Brussels.

49

935   EC, 2013. Regulation (EC) No 1306/2013 of the European Parliament and of the Council of 17

936   December 2013 on support for rural development by the European Agricultural Fund for Rural

937   Development (EAFRD) and repealing Council Regulation (EC) No 1698/2005. Official Journal

938   of the European Union, Brussels.

939   Engler R, Randin C, Thuiller W, Dullinger S, Zimmermann NE, Araújo MB, Pearman PB, Le Lay

940   G, Piedallu C, Albert CH, Choler P, Coldea G, De Lamo X, Dirnböck T, Gégout J-C, Gómez-

941   García D, Grytnes J-A, Heegaard E, Høistad F, Nogués-Bravo D, Normand S, Puşcaş M,

942   Sebastià M-T, Stanisci A, Theurillat J-P, Trivedi MR, Vittoz P, Guisan A., 2011. 21st century

943   climate change threatens mountain flora unequally across Europe. Global Change Biology 17,

944   2330-2341. https://doi.org/10.1111/j.1365-2486.2010.02393.x

945   Ernakovich, J.G., Hopping, K.A., Berdanier, A.B., Simpson, R.T., Kachergis, E.J., Steltzer, H.,

946   Wallenstein, M.D., 2014. Predicted responses of arctic and alpine ecosystems to altered

947   seasonality under climate change. Glob Chang Biol 20, 3256-3269.

948   https://doi.org/10.1111/gcb.12568

949   Fantini, A., Raffaele, F., Torma, C., Bacer, S., Coppola, E., Giorgi, F., Ahrens, B., Dubois, C.,

950   Sanchez, E., Verdecchia, M., 2018. Assessment of multiple daily precipitation statistics in ERA-

951   Interim driven Med-CORDEX and EURO-CORDEX experiments against high resolution

952   observations. Climate Dynamics 51, 877-900. https://doi.org/10.1007/s00382-016-3453-4

953   Felber R., Bretscher D., Münger A., Neftel A., Ammann C., 2016. Determination of the carbon

954   budget of a pasture: effect of system boundaries and flux uncertainties. Biogeosciences 13,

955   2959-2969. https://doi.org/10.5194/bg-13-2959-2016

956   Filippa, G., Cremonese, E., Migliavacca, M., Galvagno, M., Sonnentag, O., Humphreys, E.,

957   Hufkens, K., Ryu, Y., Verfaillie, J., di Cella, U.M., Richardson, A.D., 2015. Five years of

958   phenological monitoring in a mountain grassland: inter-annual patterns and evaluation of the

sampling protocol. Int J Biometeorol 59, 1927–1937. https://doi.org/10.1007/s00484-015-0999-5

Filippa, G., Cremonese, E., Galvagno, M., Bayle, A., Choler, P., Bassignana, M., Piccot, A., Poggio, L., Oddi, L., Gascoin, S., Costafreda-Aumedes, S., Argenti, A., Dibari, C., 2022. On the distribution and productivity of mountain grasslands in the Gran Paradiso National Park, NW Italy: A remote sensing approach. International Journal of Applied Earth Observations and Geoinformation. https://doi.org/10.1016/j.jag.2022.102718

Fitton, N., Bindi, M., Brilli, L., Cichota, R., Dibari, C., Fuchs, K., Huguenin-Elie, O., Klumpp, K., Lieffering, M., Lüscher, A., Martin, R., McAuliffe, R., Merbold, L., Newton, P., Rees, R.M., Smith, P., Topp, C.F.E., Snow, V., 2019. Modelling biological N fixation and grass-legume dynamics with process-based biogeochemical models of varying complexity. European Journal of Agronomy 106, 58-66. https://doi.org/10.1016/j.eja.2019.03.008

Fitton, N., Datta, A., Smith, K., Williams, J.R., Hastings, A., Kuhnert, M., Topp, C.F.E., Smith, P., 2014. Assessing the sensitivity of modelled estimates of N_2O emissions and yield to input uncertainty at a UK cropland experimental site using the DailyDayCent model. Nutrient Cycling in Agroecosystems 99, 119-133. https://doi.org/10.1007/s10705-014-9622-0

Fuchs, K., Merbold, L., Buchmann, N., Bellocchi, G., Bindi, M., Brilli, L., Conant, R.T., Dorich, C.D., Ehrhardt, F., Fitton, N., Grace, P., Klumpp, K., Liebig, M., Lieffering, M., Martin, R., McAuliff, R., Newton, P.C.D., Rees, R.M., Recous, S., Smith, P., Soussana, J.F., Topp, C.F.E. and Snow, V., 2020. Evaluating the potential of legumes to mitigate N_2O emissions from permanent grassland using process-based models. Global Biogeochemical Cycles 34: e2020GB006561. https://doi.org/10.1029/2020GB006561

Fuchs, K., Merbold, L., Buchmann, N., Bretscher, D., Brilli, L., Fitton, N., Topp, C.F.E., Klumpp, K., Lieffering, M., Martin, R., Newton, P.C.D., Rees, R.M., Rolinski, S., Smith, P., Snow, V.,

983   2019. Multi-model evaluation of nitrous oxide emissions from an intensively managed

984   grassland. Journal of Geophysical Research: Biogeosciences 125: e2019JG005261.

985   https://doi.org/10.1029/2019JG005261

986 Gobiet A., Kotlarski S., Beniston M., Heinrich G., Rajczak J., Stoffel M., 2014. 21st century

987   climate change in the European Alps - A review. Science of the Total Environment 493, 1138-

988   1151. https://doi.org/10.1016/j.scitotenv.2013.07.050

989 Gottfried M., Pauli H., Futschik A., Akhalkatsi M., Baranok P., Alonso J.L.B., Coldea G., Jan D.,

990   Erschbamer B., Calzado M.R.F., Kazakis G., Kraji J., Larsson P., Mallaun M., Michelsen O.,

991   Moiseev D., Moiseev P., Molau U., Merzouki A., Nagy L., Nakhutsrishvili G., Pedersen B.,

992   Pelino G., Puscas M., Rossi G., Stanisci A., Theurillat J.P., Tomaselli M., 2012. Continent-wide

993   response of mountain vegetation to climate change. Nature Climate Change 2, 111-115.

994   https://doi.org/10.1038/nclimate1329

995 Graux, A.-I., Gaurut, M., Agabriel, J., Baumont, R., Delagarde, R., Delaby, L., Soussana, J.-F.,

996   2011. Development of the Pasture Simulation Model for assessing livestock production under

997   climate change. Agriculture, Ecosystems & Environment 144, 69-91.

998   https://doi.org/10.1016/j.agee.2011.07.001

999 Hidy, D., Barcza, Z., Marjanovič, H., Ostrogovič Sever, M.Z., Dobor, L., Gelybó, Gy., Fodor, N.,

1000   Pintér, K., Churkina, G., Running, S.W. Thornton, P.E., Bellocchi, G., Haszpra, L., Horváth, F.,

1001   Suyker, A., Nagy, Z., 2016. Terrestrial ecosystem process model Biome-BGCMuSo: summary

1002   of improvements and new modeling possibilities. Geoscientific Model Development 9, 4405-

1003   4437. https://doi.org/10.5194/gmd-9-4405-2016

1004 Holman, I.P., Brown, C., Carter, T.R., Harrison, P.A., Rounsevell, M., 2019. Improving the

1005   representation of adaptation in climate change impact models. Regional Environmental Change

1006   19, 711-721. https://doi.org/10.1007/s10113-018-1328-4

1007 Jouglet, J-P., 1999. Les végétations des alpages des Alpes françaises du Sud. Guide technique pour

1008 la reconnaissance et la gestion des milieux pâturés d'altitude. Cemagref Éditions and ATEN

1009 (Atelier Technique des Espaces Naturels). (in French)

1010 Jourdain-Annequin, C., Duclos, J.-C., 2006. Aux origines de la transhumance : les Alpes et la vie

1011 pastorale d'hier à aujourd'hui. Paris: Picard. (in French)

1012 Kollas, C., Kersebaum, K.C., Nendel, C., Manevski, K., Müller, C., Palosuo, T., Armas-Herrera,

1013 C.M., Beaudoin, N., Bindi, M., Charfeddine, M., Conradt, T., Constantin, J., Eitzinger, J., Ewert,

1014 F., Ferrise, R., Gaiser, T., deCortazar-Atauri, I.G., Giglio, L., Hlavinka, P., Hoffmann, H.,

1015 Hoffmann, M.P., Launay, M., Manderscheid, M., Mary, B., Mirschel, W., Moriondo, M.,

1016 Olesen, J.E., Öztürk, I, Pacholski, A., Ripoche-Wachter, D., Roggero, P.P., Roncossek, S.,

1017 Rötter, R.P., Ruget, F., Sharif, B., Trnka, M., Ventrella, D., Waha, K., Wegehenkel, M., Weigel,

1018 H.-J., Wu, L., 2015. Crop rotation modelling – a European model intercomparison. European

1019 Journal of Agronomy 70, 98-111. https://doi.org/10.1016/j.eja.2015.06.007

1020 Kurtogullari, Y., Rieder, N. S., Arlettaz, R., Humbert, J. Y., 2020. Conservation and restoration of

1021 Nardus grasslands in the Swiss northern Alps. Applied vegetation science, 23(1), 26-38.

1022 https://doi.org/10.1111/avsc.12462

1023 Kurz, P., 2013. Management strategies and landscape diversity in commonly governed mountain

1024 pastures: a case study from Austrian Alps. European Countryside, 5(3), 212-231.

1025 https://doi.org/10.2478/euco-2013-0014

1026 Li, W., Cao, W., Wang, J., Li, X., Xu, C., Shi, S., 2017. Effects of grazing regime on vegetation

1027 structure, productivity, soil quality, carbon and nitrogen storage of alpine meadow on the

1028 Qinghai-Tibetan Plateau. Ecological Engineering 98, 123–133.

1029 https://doi.org/10.1016/j.ecoleng.2016.10.026

1030 Ma, S., Lardy, R., Graux, A-I., Ben Touhami, H., Klumpp, K., Martin, R., Bellocchi, G., 2015.

1031 Regional-scale analysis of carbon and water cycles on managed grassland systems.

1032 Environmental   Modelling   &   Software   72,   356-371.

1033 https://doi.org/10.1016/j.envsoft.2015.03.007

1034 Mathieu, J., 2000. Storia delle Alpi 1500-1900: Ambiente, sviluppo e società (volume 4).

1035 Bellinzona: Casagrande. (in Italian)

1036 Melo Damian, J., da Silva Matos, E., Carneiro e Pedreira, B., de Faccio Carvalho, P.C., Premazzi,

1037 L.M., Williams, S., Paustian, K., Pellegrino Cerri, C.E., 2021. Predicting soil C changes after

1038 pasture   intensification   and   diversification   in   Brazil.   Catena   202:   105238.

1039 https://doi.org/10.1016/j.catena.2021.105238

1040 Moreau, J.C., Lorgeou, J., 2007. First elements for a prospective study of the effects of climatic

1041 changes on pastures, maize and the forage systems. Fourrages Journée de l'A.F.P.F. (Association

1042 Française pour la Production Fourragère), 191, pp 285-295, 11 p ; ref : 1/4 p, ISSN 0429-2766

1043 Moss, R.H., Edmonds, J.A., Hibbard, K.A., Manning, M.R., Rose, S.K., van Vuuren, D.P., Carter,

1044 T.R., Emori, S., Kainuma, M., Kram, T., Meehl, G.A., Mitchell, J.F, Nakicenovic, N., Riahi, K.,

1045 Smith, S.J., Stouffer, R.J., Thomson, A.M., Weyant, J.P., Wilbanks, T.J., 2010. The next

1046 generation of scenarios for climate change research and assessment. Nature 463, 747-756.

1047 https://doi.org/10.1038/nature08823

1048 Nabat, P., Somot, S., Cassou, C., Mallet, M., Michou, M., Bouniol, D., Decharme, B., Drugé, T.,

1049 Roehrig, R., Saint-Martin, D., 2020. Modulation of radiative aerosols effects by atmospheric

1050 circulation over the Euro-Mediterranean region. Atmospheric Chemistry and Physics 20, 8315-

1051 8349. https://doi.org/10.5194/acp-20-8315-2020

1052 Necpálová, M., Anex, R.P., Fienen, M.N., del Grosso, S.J., Castellano, M.J., Sawyer, J.E., Iqbal,

1053 J., Pantoja, J.L., Barker, D.W., 2015. Understanding the DayCent model: calibration, sensitivity,

1054   and identifiability through inverse modeling. Environmental Modelling & Software 66, 110-

1055   130. https://doi.org/10.1016/j.envsoft.2014.12.011

1056 Negro, M., Rolando, A., Palestrini, C., 2011. The impact of overgrazing on dung beetle diversity

1057   in the Italian Maritime Alps. Environmental Entomology 40, 1081–1092.

1058   https://doi.org/10.1603/EN11105

1059 Nettier, B., Dobremez, L., Coussy, J.L., Romagny, T., 2010. Attitudes of livestock farmers and

1060   sensitivity of livestock farming systems to drought conditions in the French Alps. Journal of

1061   Alpine Research 98-4. http://rga.revues.org/index1294.html

1062 Nori S., Gemini M., 2011. The Common Agricultural Policy vis-à-vis European pastoralists:

1063   principles and practices. Pastoralism: Research, Policy and Practice 1: 27.

1064   https://doi.org/10.1186/2041-7136-1-27

1065 Parton, W.J., Hartman, M., Ojima, D., Schimel, D., 1998. DAYCENT and its land surface

1066   submodel: description and testing. Global and Planetary Change 19, 35-48.

1067   https://doi.org/10.1016/S0921-8181(98)00040-X

1068 Parton, W.J., Schimel, D.S., Ojima, D., Cole, C.V., 1994. A general model for soil organic matter

1069   dynamics: sensitivity to litter chemistry, texture and management. In: Bryant, R.B., Arnoldm,

1070   R.W. (Eds.), Quantitative modeling of soil forming processes. Soil Science Society of America,

1071   Madison, pp 147–167. https://doi.org/10.2136/sssaspecpub39.c9

1072 Philip, J.R., 1993. Variable-head ponded infiltration under constant or variable rainfall. Water

1073   Resources Research 29, 2155–2165. https://doi.org/10.1029/93WR00748

1074 Piccot, A., Argenti, G., Bellocchi, G., Brien, P., Cremonese, E., Della-Vedova, M., Dibari, C,

1075   Galvagno, M., Ghidotti, S., Napoléone, C., Stendardi, L., Targetti, S., Trombi, G., Varese, P.,

1076   Bassignana, M., 2022. Adaptation policies and measures to cope with climate change in Alpine

mountain farming. Proceedings. ISCRAES (International Symposium on climate-resilient agri-environmental systems) Dublin, 28-31 August 2022

Pielke, R., Ritchie, J. 2021. Distorting the view of our climate future: The misuse and abuse of climate pathways and scenarios. Energy Research & Social Science 72, 101890. https://doi.org/10.1016/j.erss.2020.101890

Pinares-Patiño, C.S., D'Hour, P., Jouany, J.-P., Martin, C., 2007. Effects of stocking rate on methane and carbon dioxide emissions from grazing cattle. Agriculture, Ecosystems and Environment 121, 30–46. https://doi.org/10.1016/j.agee.2006.03.024

Pulina, A., Lai, R., Salis, L., Seddaiu, G., Roggero, P.P., Bellocchi, G., 2018. Modelling pasture production and soil temperature, water and carbon fluxes in Mediterranean grassland systems with the Pasture Simulation model. Grass and Forage Science 73, 272-283. https://doi.org/10.1111/gfs.12310

Richter, K., Atzberger, C., Hank, T.B., Mauser, W., 2012. Derivation of biophysical variables from Earth observation data: validation and statistical measures. Journal of Applied Remote Sensing 6: 063557. https://doi.org/10.1117/1.JRS.6.063557

Riedo, M., Grub, A., Rosset, M., Fuhrer, J., 1998. A Pasture Simulation model for dry matter production, and fluxes of carbon, nitrogen, water and energy. Ecological Modelling 105, 141-183. https://doi.org/10.1016/S0304-3800(97)00110-5

Rousselot, M., Durand, Y., Giraud, G., Mérindol, L., Dombrowski-Etchevers, I., Déqué, M., & Castebrunet, H., 2012. Statistical adaptation of ALADIN RCM outputs over the French Alps - application to future climate and snow cover. The Cryosphere 6, 785-805. https://doi.org/10.5194/tc-6-785-2012

Ruti, P.M., Somot, S., Giorgi, F., Dubois, C., Flaounas, E., Obermann, A., Dell'Aquila, A., Pisacane, G., Harzallah, A., Lombardi, E., Ahrens, B., Akhtar, N., Alias, A., Arsouze, T., Aznar,

1101   R., Bastin, S., Bartholy, J., Béranger, K., Beuvier, J., Bouffies-Cloché, S., Brauch, J., Cabos,

1102   W., Calmanti, S., Calvet, J.-C., Carillo, A., Conte, D., Coppola, E., Djurdjevic, V., Drobinski,

1103   P., Elizalde-Arellano, A., Gaertner, M., Galàn, P., Gallardo, C., Gualdi, S., Goncalves, M.,

1104   Jorba, O., Jordà, G., L'Heveder, B., Lebeaupin-Brossier, C., Li, L., Liguori, G., Lionello, P.,

1105   Maciàs, D., Nabat, P., Önol, B., Raikovic, B., Ramage, K., Sevault, F., Sannino, G., Struglia,

1106   M.V., Sanna, A., Torma, C., Vervatis, V., 2016. Med-CORDEX initiative for Mediterranean

1107   climate studies. Bulletin of the American Meteorological Society 97, 1187-1208.

1108   https://doi.org/10.1175/BAMS-D-14-00176.1

1109   Sándor, R., Barcza, Z., Acutis, M., Doro, L., Hidy, D., Köchy, M., Minet, J., Lellei-Kovács, E.,

1110   Ma, S., Perego, A., Rolinski, S., Ruget, F., Sanna, M., Seddaiu, G., Wu, L., Bellocchi, G., 2017.

1111   Multi-model simulation of soil temperature, soil water content and biomass in Euro-

1112   Mediterranean grasslands: Uncertainties and ensemble performance. European Journal of

1113   Agronomy 88, 22-40. https://doi.org/10.1016/j.eja.2016.06.006

1114   Sándor, R., Picon-Cochard, C., Martin, R., Louault, F., Klumpp, K., Borras, D., Bellocchi, G.,

1115   2018. Plant acclimation to temperature: Developments in the Pasture Simulation model. Field

1116   Crops Research 222, 238-255. https://doi.org/10.1016/j.fcr.2017.05.030

1117   Shen, M., Piao, S., Cong, N., Zhang, G., Janssens, I.A., 2015a. Precipitation impacts on vegetation

1118   spring phenology on the Tibetan Plateau. Glob. Change Biol. 21, 3647-3656.

1119   https://doi.org/10.1111/gcb.12961

1120   Soudani, K., Hmimina, G., Delpierre, N., Pontailler, J.Y., Aubinet, M., Bonal, D., Caquet, B., de

1121   Grandcourt, A., Burban, B., Flechard, C., Guyon, D., Granier, A., Gross, P., Heinesh, B.,

1122   Longdoz, B., Loustau, D., Moureaux, C., Ourcival, J.M., Rambal, S., Saint André, L., Dufrêne,

1123   E., 2012. Ground-based network of NDVI measurements for tracking temporal dynamics of

1124   canopy structure and vegetation phenology in different biomes. Remote Sensing of Environment

1125   123, 234-245. https://doi.org/10.1016/j.rse.2012.03.012

1126   Stendardi, L, Dibari, C., Bassignana, M., Bindi, M., Brilli, L., Choler, P., Cremonese, E., Filippa,

1127   G., Piccot, A., Argenti, G., 2022. Pasture areas in the Gran Paradiso National Park. Journal of

1128   Maps. https://doi.org/10.1080/17445647.2022.2120835

1129   Targetti, S., Mouléry, M., Napoléone, C., 2019. Agricultural policy, climate change adaptation and

1130   sustainability: Assessing drivers and mechanisms in an alpine case study area. Contributed paper

1131   at the 8th AIEAA (Italian Association of Agricultural and. Applied Economics) Congress, 13-

1132   14 June, Pistoia, Italy. https://www.aieaa.org/aieaaconference2019

1133   Van Oijen, M., Barcza Z., Confalonieri R., Korhonen P., Kröel-Dulay G., Lellei-Kovács E., Louarn

1134   G., Louault F., Martin R., Moulin T., Movedi E., Picon-Cochard C., Rolinski S., Viovy N.,

1135   Wirth S.B., Bellocchi, G., 2020. Incorporating biodiversity into biogeochemistry models to

1136   improve prediction of ecosystem services in temperate grasslands: review and roadmap.

1137   Agronomy 10: 259. https://doi.org/10.3390/agronomy10020259

1138   Van Vuuren, D.P., Edmonds, J., Kainuma, M., Riahi, K., Thomson, A., Hibbard, K., Hurtt, G.C.,

1139   Kram, T., Krey, V., Lamarque, J.-F., Masui, T., Meinshausen, M., Nakicenovic, N., Smith, S.J.,

1140   Rose, S.K., 2011. The representative concentration pathways: an overview. Climatic Change

1141   109, 5-31. https://doi.org/10.1007/s10584-011-0148-z

1142   Vital, J.A., Gaurut, M., Lardy, R., Viovy, N., Soussana, J.F., Bellocchi, G., Martin, R., 2013. High-

1143   performance computing for climate change impact studies with the Pasture Simulation model.

1144   Computers   and   Electronics   in   Agriculture   98,   131-135.

1145   https://doi.org/10.1016/j.compag.2013.08.004

1146 Volaire, F., Lelièvre, F., 2001. Drought survival in *Dactylis glomerata* and *Festuca arundinacea*

1147 under similar rooting conditions. Plant and Soil 229, 225-234.

1148 https://doi.org/10.1023/A:1004835116453

1149 Wanner, A., Pröbstl-Haider, U., Feilhammera, M., 2021. The future of Alpine pastures -

1150 Agricultural or tourism development? Experiences from the German Alps. Journal of Outdoor

1151 Recreation and Tourism 35: 100405. https://doi.org/10.1016/j.jort.2021.100405

1152 Weitz, A.M., Grauel, W.T., Keller, M., Veldkamp, E., 1997. Calibration of time domain

1153 reflectometry technique using undisturbed soil samples from humid tropical soils of volcanic

1154 origin. Water Resources Research 33, 1241-1249. https://doi.org/10.1029/96WR03956

1155 Wilcke, R.A., Bärring L., 2016. Selecting regional climate scenarios for impact modelling studies.

1156 Environmental Modelling & Software 78, 191-201.

1157 https://doi.org/10.1016/j.envsoft.2016.01.002

1158 Wu, W., Geller, M.A., Dickinson, R.E., 2002. A case study for land model evaluation: Simulation

1159 of soil moisture amplitude damping and phase shift. Journal of Geophysical Research 107, ACL

1160 20-1-ACL 20-13. https://doi.org/10.1029/2001JD001405

1161 Xu, C., Liu, H., Williams, A.P., Yin, Y., Wu, X., 2016. Trends toward an earlier peak of the

1162 growing season in Northern Hemisphere mid-latitudes. Glob. Chang. Biol. 22, 2852–2860.

1163 https://doi.org/10.1111/gcb.13224

1164 Zeeman, M.J., Hiller, R., Gilgen, A.K., Michna, P., Plüss, P., Buchmann, N., Eugster, W., 2010.

1165 Management and climate impacts on net CO_2 fluxes and carbon budgets of three grasslands

1166 along an elevational gradient in Switzerland. Agricultural and Forest Meteorology 150, 519–

1167 530. https://doi.org/10.1016/j.agrformet.2010.01.011

1168   Zeeman, M.J., Shupe, H., Baessler, C., Ruehr, N.K., 2019. Productivity and vegetation structure of

1169   three differently managed temperate grasslands. Agriculture, Ecosystems and Environment

1170   270–271, 129–148. https://doi.org/10.1016/j.agee.2018.10.003